Matīss Maltisovs

OPERATING METHODS OF HIGH VOLTAGE BISTABLE SMART GLASS ELECTRONICS SYSTEMS

Doctoral Thesis

RIGA TECHNICAL UNIVERSITY

Faculty of Electronics and Telecommunications

Institute of Radioelectronics

Matīss Maltisovs

Doctoral Student of the Study Programme "Electronics"

OPERATING METHODS OF HIGH VOLTAGE BISTABLE SMART GLASS ELECTRONICS SYSTEMS

Doctoral Thesis

Scientific supervisor
Assoc. Professor *Dr. sc. ing.*
DMITRIJS PIKUĻINS

Maltisovs M. Operating Methods of High Voltage Bistable Smart Glass Electronics Systems. Doctoral Thesis. – Riga: RTU Press, 2022. – 89 pages.

DOCTORAL THESIS PROPOSED TO RIGA TECHNICAL UNIVERSITY FOR THE PROMOTION TO THE SCIENTIFIC DEGREE OF DOCTOR OF ENGINEERING SCIENCES

To be granted the scientific degree of Doctor of Engineering Sciences (*Ph. D*), the present Doctoral Thesis has been submitted for the defence at the open meeting of RTU Promotion Council on March 11, 2022 at the Faculty of Electronics and Telecommunications of Riga Technical University, Āzenes street 12, room 201.

OFFICIAL REVIEWERS

Asoc. Professor *Dr. sc. ing.* Andis Supe
Riga Technical University

Professor *Dr. phys.* Mārtiņš Rutkis
University of Latvia, Institute of Solid State Physics

Professor *Ph. D.* Timothy D. Wilkinson
University of Cambridge, Great Britain

DECLARATION OF ACADEMIC INTEGRITY

I hereby declare that the Doctoral Thesis submitted for the review to Riga Technical University for the promotion to the scientific degree of Doctor of Engineering Sciences is my own. I confirm that this Doctoral Thesis had not been submitted to any other university for the promotion to a scientific degree.

Matiss Maltisovs .... (signature)
Date: ....

Doctoral Thesis has been written in English. It consists of an Introduction; 7 chapters; Conclusions; 50 figures; 10 tables; the total number of pages is 89. The Bibliography contains 154 titles.

DEDICATION

To my wife Rūta

and my both sons Krišjānis and Mārtiņš

ACKNOWLEDGEMENTS

ANNOTATION

Liquid crystal displays ($LCDs$) have been used by mankind on a daily basis for decades, but the demand for their integration and development of new products is only growing. One of the research directions is smart glass/windows, and, although they are known for more than 25 years, there are areas that still need to be researched. This Thesis focuses on *Smectic-A* (*SmA*) liquid crystals' (*LCs*) functional behaviour in order to understand if this will be the next generation product, that could improve society's daily life.

An in-depth literature review discusses existing studies, obtained experimental data and attempts to develop functional products. The main unresolved problems are highlighted, described in detail and solutions are offered.

The *SmA LC* is able to maintain two stable optical states: transparent and light scattering, without additional energy resources, allowing to save electricity costs. The optical properties of this liquid crystal are by far the best compared to the products available in the market, i. e. the light transmittance in transparent state is 85+ % and in scatter state $<$ 2 %. Enabling the *LC* to be used for a variety of purposes, such as smart windows to scatter light on a sunny day or provide a sense of privacy in an open type office space.

In order to understand the potential of *SmA LC* in the smart glass/window technology, analysis of existing products was performed, a summary of an active smart glass/windows provided and a comparative study between them was made. In addition, an in-depth study of long-term functional stability was performed, during which the most popular types of defects were listed and analysed. Solutions for defect elimination and recommendations for optimization of switching systems and production processes are provided. A methodology for determining the electrical parameters of an *LC* has been developed in order to create an electrical simulation model and facilitate the development of electronic switching systems.

The results of the work are summarized and recommendations for the functional use of *SmA LCs* of various designs and sizes are provided.

CONTENTS

LIST OF SYMBOLS AND ABBREVIATIONS

LCD	Liquid crystal display
SmA	*Smectic-A* liquid crystal
LC	Liquid crystal
TV	Television
EC	Electrochromic device
PDLC	Polymer dispersed liquid crystal device
SPD	Suspended particle device
UV	Ultraviolet light
ITO	Indium tin oxide
SiO$_2$	Silicon dioxide
Ns	Nematic liquid crystals
Ss	Smectic liquid crystals
n(r)	Unit vector, r — space coordinate, determines preferred molecule orientation
Sc	*Smectic-C* liquid crystal
ChLC	Cholesteric liquid crystal
Chiral	Unique ability to selectively reflect one component of circularly polarized light
ε	*LC* cell dielectric material coefficient
IR	Infrared light
η$_o$	Ordinary refractive index
η$_p$	Polymer refractive index
RMS	Root mean square of measured voltage or consumed power
PVD	Physical vapour deposition
LiCoO$_2$	Lithium cobalt oxide
WO$_3$	Polycrystalline tungsten oxide
Ω/sq	ITO resistance value
PC	Personal computer
OPMP	Optical parameter measurement platform
AHV	Alternating high voltage source
E24 standard	System of preferred numbers (also called preferred values) derived for use in electronic components
Wh	Watt-hours
PDT	Product development testing
HALT	Highly accelerated life testing
QT	Qualification tests
FOAT	Failure oriented accelerated testing

BIT	Burn in test
PVC	Polyvinyl chloride, synthetic plastic polymer used for window frame manufacturing
RC	Resistor—capacitor circuit
C_{LC}	Liquid crystal capacitance
R_S	LC cell series resistance (ITO resistance)
R_P	LC cell parallel resistance (LC resistance)
Q_C	Capacitor charge (LC cell charge)
V_S	Supplied voltage
E	Electric field intensity
E_{br}	LC electrical breakdown value
ICT	Information and communication technology
VATP	Ventspils high technology park
SGD	Smart glass driver
2D	Two dimensional

1. GENERAL DESCRIPTION OF THE THESIS

1.1. Introduction

Nowadays Liquid crystal display (LCD) is an integral part of humans' everyday life. High demand for new and innovative LCD products force industry to develop and implement new types of $LCDs$. They are used in everything starting from smartphones and Television (TV) sets to washing machines. Liquid crystals (LCs) have far wider applications, one of them — smart or switchable glass, having voltage dependent optical properties which can be altered by application of specific electrical signals.

Smart glass technology has been studied for the last few decades; however, its demand is gathering innovation in raw materials, technologies and the possibilities for new applications across various sectors, e. g. smart windows.

Windows serve an important function in homes and commercial buildings. They let the light in and brightens the room, saving electricity costs. They provide heat and air conditioning, and other appliances must be used in order to adjust the comfort level. But windows are not the best insulating material for the cold season, and they are not something people typically associate with being a cutting-edge technology.

There are two primary types of smart glass, defined by whether or not their changeability requires an electrical signal:
- **Active devices (depends on the signal):**
    - Electrochromic (EC)
    - Polymer Dispersed Liquid Crystal ($PDLC$)
    - Suspended Particle Devices (SPD)
    - Other (e. g. bistable $Smectic$-A (SmA) LC devices)
- **Passive devices (does not depend on signal):**
    - Thermochromic
    - Photochromic

The main advantages of the smart glass are:
- **privacy** – a fast state change from clear to light scattering state and vice versa, low transmittance in opaque state, ability to replace curtains, shutter blinds, drapes;
- **cost savings** – no need for an additional cleaning equipment, saves costs for heating, air-conditioning and lighting, no costs of installing and maintaining motorized light screens, blinds or curtains;
- **ultraviolet (UV) protection** – blocks > 98 % of UV rays;
- **display and advertising** – can be used as a projection screen when switched to the light scattering state.

SmA LC cells have attained considerable attention to be one of the most promising devices for smart glass applications due to long term bistability (very high LC viscosity), low haze at clear state, low transmittance at scatter state and low power consumption.

However, along with many advantages, only several engineering related research papers have been published, i. e., most of the studies are based on LC, its compounds, chemical or physical processes:

- First *Smectic-A LC* studies started to appear in the 1970s where the main interest was focused on molecular model and order [1], [2], phase and magnetic transitions [3], [4], ultrasound propagation [5], light scattering [6], [7], viscous flow [8], electric field effects [9] and first molecule reorientation defect review [10].

- The next decade was marked by technological developments that allowed the production of the first LCD samples. In parallel with LC research, engineering research is beginning to emerge, i. e., analytic solution of the heat-flow equation applied to LCD panel [11], LCD matrix-addressing with thermal and electric field effects [12], [13], [14], [15], first LC panels for television projection systems [16], [17], electrode configurations for power consumption and contrast enhancements [18], flat panel, colour image displays [19], [20], [21] and the soft-mode ferroelectric effect (sub-microsecond electro-optic switching) [22].

- Although the first LCD samples were created in the 1980s, the technical support was insufficient to realize the production of different size LC panels. Therefore, the greatest emphasis was placed on chemical or physical processes, i. e., x-ray diffraction on LC cells, materials [23], [24], [25], LC polymers, phase transitions and different materials [26], [27], [28], [29], [30], [31], analysis of destructive physicochemical processes [32] and optical distortion of LCD pixels [33]. Engineering research continues on electro-optic effect [34], operating, switching characteristics [35], [36], electrohydrodynamic instability [37], thermally and electrically controllable light-scattering effect [38], [39], first studies start to appear about polymer dispersed liquid crystal ($PDLC$) films [40], [41].

- The first decade of the new century (2000s) marked an increased interest in applied physics, i. e., LC realignment, electric field, temperature, depth and random environment analysis with x-ray diffraction [42], [43], [44], [45]. There was also a growing interest in chemical processes, more precisely, studies with new LC mixtures using organosiloxane [46], [47], LC polymers, structure effects and degradation boundaries [48], [49], [50], [51]. With the development of industrial performance, engineering research topics become more diverse, i. e., two-direction electric field driving [52], electro-optic control features [53], [54], [55], [56] as well as temperature influence on switching [57]. Development leads to the emergence of new types of $LCDs$ - flexible and reflective displays [58], [59], [60], [61], [62], first studies appear about switchable glazing theme [63] and manufacturing research - adsorption processes during the filling of a display [64].

- Over the last ten years, interest in SmA LC devices has declined compared to the period 1980-2000. However, bistable LCD types/modes are summarized in handbook chapter [65], electro-optic effects in thermotropic liquid crystals published

in a book [66]. Engineering related studies have emerged in outdoor product applications [67], [68], [69], [70], electric breakdown of dielectric thin films [71], experiments with photolithography and photoinduced phase separation to create flexible device [72]. Also other research fields are interested in electrode structure and hybrid surface treatment [73], optical fibre lasing and waveguiding [74], focal conic studies [75], [76].

Over the past 50 years, many different studies have been conducted on and around SmA LC and their devices. Despite rapid technological development, SmA $LCDs$ have not reached the market compared to other similar products such as $PDLC$. This begs the question: why?

- Existing studies do not provide detailed information about the conducted sample size, however in most cases it was $< 50 \times 50$ mm. This means that regardless of the technological possibilities, no technical solution has been found to successfully produce SmA LC devices of different sizes, i. e., such as 8×8 mm up to 300×400 mm or bigger.

- The driving methodology is discussed quite extensively, i. e., matrix-addressing with thermal and electric field effects [14], [15], electrode configurations [18], operating, switching characteristics [35], [36], electrohydrodynamic [37], etc. None of the studies fully addresses switching threshold frequencies for both states (light scattering and transparent) and from state to state. Also the frequency dependence of the switching speed and or light transmission is unknown.

- In addition to LC switching, specific issues are addressed, such as the use of different frequencies and signal amplitudes to obtain different levels of grey tones in a light scattering state. But the topics of switching sequence, pauses between state-state, pixel-pixel switching, their effect on light transmittance, etc. are not covered.

- No information is available about long term switching problems, defects. As well as no studies about LC defect analysis have been published, not to mention to finding solutions to resolve defects or prevent their appearance.

- Lack of theoretical studies and experiments to obtain an equivalent load model, i. e., to be able to replicate the LCD in electronic simulation environments with equivalent load, which would help to speed up the electronic design process of desired product more efficiently without iterative approaches and testing with real samples with high production costs.

- It is not known how the power consumption changes in relation to the area to be driven or the amount of the current required to switch an area of a certain LCD or pixel size. What is the power consumption for different LC cell types, designs?

- There is no information about differences in the thickness of the protective coatings, such as SiO_2, effect the switching speed, light transmittance, power consumption. Also, what is the effect on changes in indium tin oxide (ITO) resistance etc.?

1.2.   Objectives of the Thesis

The purpose of this Thesis is to explore operational and electrical properties of the $SmA\ LC$ cells, as well as gain an in-depth understanding of functional long-term stability. To achieve the goal, the following objectives have to be fulfilled:

- Explore the light transmittance and switching speed of $SmA\ LC$ cells, depending on the switching frequency (Chapter 3, Section 3.2);
- Explore power consumption based on switching area (Chapter 3, Section 3.3);
- Explore switching differences between different LC cell design types (Chapter 4, Section 4.5);
- Explore equivalent load representation options for electronic sub-system simulations (Chapter 6, Sections 6.2-6.4);
- Explore LC defect types, their appearance reasons and possible solutions (Chapter 4 and 5).

Other active smart glass devices should be explored by reviewing and analysing other research topics on electrical and optical functionality, so they could be compared with $SmA\ LC$ devices.

1.3.   Scientific novelty and main results

The following list outlines the major contributions that have been made during writing this Doctoral Thesis:

- New capillary filling process was developed that successfully allows to fill different size (from 10×10 mm up to 300×400 mm) $SmA\ LC$ cells.
- Optical parameter measurement platform ($OPMP$) and switching matrix devices was developed that are able to measure light transmittance, switching speed, viewing angle and switch up to 5 different design, type $SmA\ LC$ cells to increase testing volume for future needs.
- For the first time $SmA\ LC$ cell frequency response and its dependence on switching speed, light transmittance and power consumption has been studied.
- For the first time $SmA\ LC$ cell equivalent load theoretical model approach has been studied.
- For the first time $SmA\ LC$ cell long-term switching defect analysis has been performed.
- For the first time $SmA\ LC$ cell defect resolving methodology has been proposed and tested (approbated).
- Industrial type $SmA\ LC$ driver was designed with capability to simultaneously switch two LC cells in size up to 300×400 mm.

1.4.   Theses to be defended

- It is possible to obtain in 300×400 mm $SmA\ LC$ cell the parameters required for smart glass applications — light transmittance $> 85\ \%$ and switching speed < 150 ms in transparent state, light transmittance $< 2\ \%$ and switching speed < 1700 ms in scatter state by applying 100—240 V > 0.9 A DC balanced square wave control signal within 20—40 Hz range for transparent state and within 400—700 Hz range for scatter state.

- During long-term functional testing, switching > 1000 times between both optical states, the following visual defects appear in $SmA\ LC$ cell, preventing further use in smart glass applications: non uniform active area, pronounced laser ablation lines, random LC clusters, wavy pixels' outline and rugged pixels' edges.

- Long-term functionality and visual stability of $SmA\ LC$ cells could be improved by: switching parameter and sequence optimization — additional 1—5 s pauses in-between state-state, pixel-pixel switching; changing control signal to DC balanced sine wave, as well as temperature treatment, but trade-off must be found between visual performance, functional switching and complexity of electronics design.

- The performance of the SmA liquid crystals can be modelled with the experimentally obtained equivalent load theoretical model: $RS = 71\ \Omega$, $RP = 13$ kΩ, $C = 53$ nF, to understand electric functionality of 300×400 mm $SmA\ LC$ cells within 100—240 V range, which can be adjusted to other sizes.

1.5.   Approbation

The following papers have been published in scientific journals & conference proceedings:

- M. Maltisovs, K. Krumins, A. Ozols, and D. Pikulins, "Study of the Operational Properties of Bistable Smectic-A Liquid Crystal Displays", *Latvian Journal of Physics and Technical Sciences*, vol. 55, no. 3, pp. 54—62, 2018, doi: 10.2478/lpts-2018-0021. (**Scopus**)

- M. Maltisovs and D. Pikulins, "Study of Electrical Properties of Bistable Smectic-A Liquid Crystal Displays", *Latvian Journal of Physics and Technical Sciences*, vol. 56, no. 5, pp. 3—11, 2019, doi: 10.2478/lpts-2019-0026. (**Scopus**)

- M. Maltisovs, K. Krumins, A. Ozols, and D. Pikulins, "Identifying Defects in Bistable Smectic-A Liquid Crystal Displays After Extended Period of Functional Testing", *2020 IEEE 61st International Scientific Conference on Power and Electrical Engineering of Riga Technical University (RTUCON)*, Riga, Latvia, 2020, pp. 1—5, doi: 10.1109/RTUCON51174.2020.9316559. (**IEEE Xplore**)

- M. Maltisovs, K. Krumins, A. Ozols, and D. Pikulins, "Resolving Defects in Bistable Smectic-A Liquid Crystal Displays", *2020 IEEE 3rd International Conference on Automation, Electronics and Electrical Engineering (AUTEEE)*, Shenyang, China, 2020, pp. 243-247, doi: 10.1109/AUTEEE50969.2020.9315707. (**IEEE Xplore**)
Author has presented the obtained results in the following scientific conferences:
- International Scientific Conference of Environmental and Climate Technologies – **CONECT 2020**, Riga, Latvia, May 13-15, 2020.
- IEEE 61st International Scientific Conference on Power and Electrical Engineering of Riga Technical University – **RTUCON 2020**, Riga, Latvia, November 5—7, 2020.
- IEEE 3rd International Conference on Automation, Electronics and Electrical Engineering – **AUTEEE 2020**, Shenyang, China, November 20—22, 2020.

1.6.   Structure of the Thesis

The doctoral thesis contains 7 chapters and 4 appendices, the total amount of pages 89:
- chapter 1 — general description of the work, scientific novelties, main results, approbation and theses to be defended;
- chapter 2 — brief introduction about *LCs*, description of smart glass devices and comparison of their electro-optical characteristics;
- chapter 3 — *SmA LC* cell operational properties, experimentally obtained results of frequency response, switching speed, light transmittance and power consumption compared side by side;
- chapter 4 — *SmA LC* cell functional testing for extended period of time, identification, review and analysis of the most common defects that appeared during and were detected after the testing;
- chapter 5 — defect resolving methods and driving waveform optimization to further improve overall functionality and visual looks of *SmA LC* cells;
- chapter 6 — *SmA LC* cell electrical properties, theoretical approach to model *LC* characteristics: series, parallel resistance and *LC* capacitance;
- chapter 7 — created products, i. e., different design light shutters, smart windows, numeric signs, as well as testing and functional equipment for *SmA LC* cells;
- chapter 8 — conclusion of the Doctoral Thesis, suggestions for future research directions and development, as well as functional parameters are provided for different design *SmA LC* cells to achieve most pleasant visual looks and best functional performance.
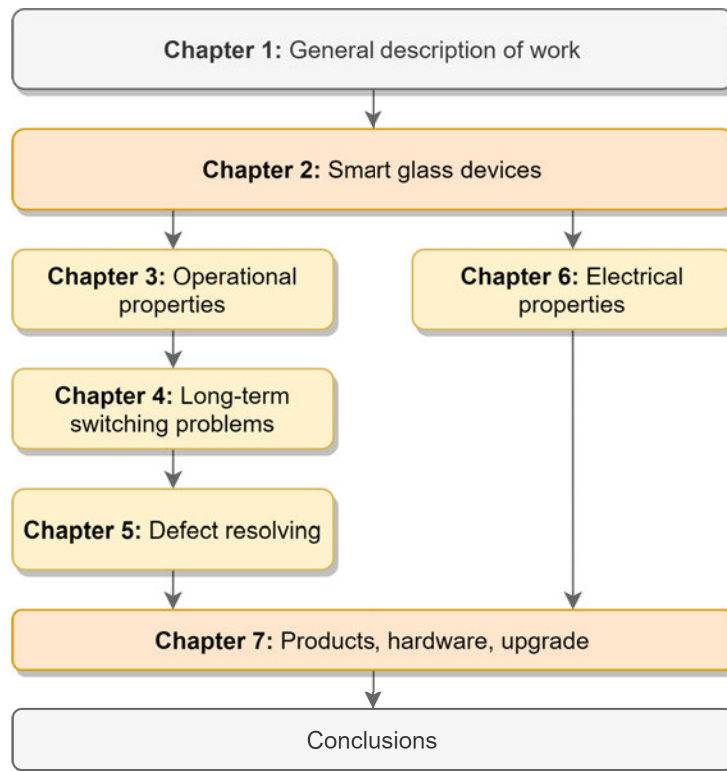
Fig. 1.1. The outline of the Doctoral Thesis.

2.   SMART GLASS DEVICES

2.1.   Objective and tasks

In this chapter *LCs*, as well as active smart window devices will be reviewed. Information about bistable *SmA LC* cell properties is provided, to be able to compare electro-optical characteristics of all active smart glass devices.

In order to meet the objective the following tasks have to be fulfilled:

- Review of:
    - *LCs*, brief history, differences between *LC* types, molecular order, etc.;
    - polymer dispersed liquid crystal devices;
    - suspended particle devices;
    - electrochromic devices;
    - *SmA LC* cells, provide information about manufactured unit physical, chemical, electrical properties;
    - active smart glass device electro-optical characteristics.

2.2.   Introduction of *LCs*

Solid, liquid and gaseous states were the only known states of matter before the discovery of *LCs*. A solid matter can be either crystalline of amorphous. When solid is heated above its melting point, it turns into an isotropic liquid having neither positional nor orientational order, which, after cooling, turns back into solid.

The *LCs* were discovered in 1888 by Friedrich Reinitzer [77]. The intensive study of LC state, brought to a great number of publications and books in this field of the science. Detailed study of *LCs* began in the 1970s when the significance of *LCs* for technology (electro-optical devices, thermography) was shown. Excellent collection of fundamental documents in the field can be found here [78] and update version - recent developments and the future perspectives in physics of *LCs* here [79].

The liquid crystal (mesophase, mesomorphic state of the matter, anisotropic liquid) is matter in state intermediate between solid crystal and isotropic liquid (see Figure 2.1). The fundamental property characterizing the liquid crystal state is the physical (optical, electrical and magnetic) anisotropy, like that in the solid crystals. At the same time these materials exhibit the mechanical properties of the conventional isotropic liquids-fluidity, capillarity, drop formation. Physical *LCs* properties studies can be found here [80], [81], optical and electro-optical properties are specifically discussed in [82], [83].
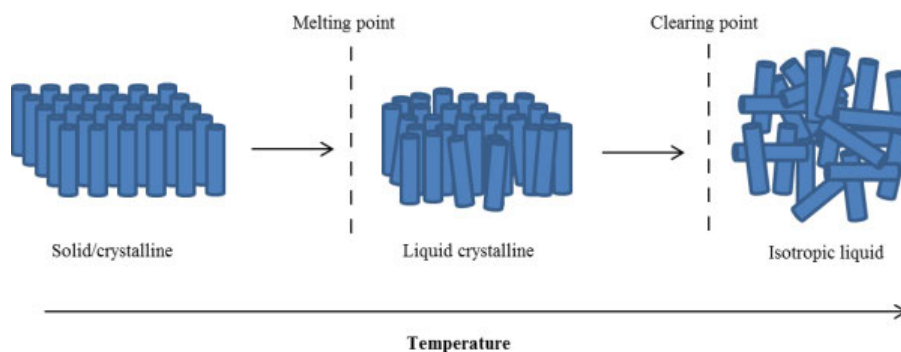
Fig. 2.1. Rod-like (calamitic) molecules representing molecular arrangement of thermotropic liquid crystalline phase transitions [84].

An important factor determining the mesophase appearing, turn out the geometric anisotropy of the molecule. The figure of the molecular rotation around the long molecular axis must be with form of cylinder where the ratio of the height to the diameter is big enough. The single molecule, however, does not possess liquid crystal properties yet, but is able to aggregate with other molecules thus creating ordered structure. Namely this ability, called mesogenity, appears as property of the liquid crystal compounds. Both, geometrical and aggregation abilities of the molecule ensure the passage of the system across the one or more mesophases before the transition to the isotropic liquid.

The transition between the intermediate states could be provoked either by pure thermal (thermotropic LCs) or by concentration (lyotropic LCs) variations. Thus depending on the molecular form, on the temperature, solvents, etc., one can observe variety of phenomena and transitions in the LC materials. The liquid crystal state can be formed: 1 - using rods that either occur naturally or can be made up artificially; 2 - with polymers; 3 - with more complex units that are associated structures of molecules and ions [80], [85].

The type of the liquid crystals depends significantly on the structure of molecules or groups of molecules. Majority of the known LCs compounds contains one or a few benzene rings, constituting the molecular part, which defines the basic physical properties of the mesophase and realizes the two states [86], [87]:

- **nematics (Ns)** characterized by a high long range order degree and absence of long range translation order, meaning that the long molecular axes spontaneously orient approximately parallel to each other, while the centers of gravity of the molecules have no long range order. For the description of the molecular axis long range order (the macroscopic state of the nematic liquid) one initiates, in each LC system point, called director (unit vector n(r), r - space coordinate). n determines a preferred molecular orientation, along which the molecular axis are in average oriented. In the uniaxial nematics: n and -n are equivalent; all physical properties depend only on quadratic combination of the n components; such LC is not polar.

19

- **smectics (Ss)** - the smectic liquid crystals consist of planar layers freely shifting one toward other, situated on an equal distance between them. They are characterized by one-dimensional order in three dimensions: such system can be viewed as a set of two-dimensional liquid layers stacked on each other. The distance between the layers is well defined - interlayer spacing. In each layer the molecules are oriented in the preferable direction (translation long range order), but the centers of the molecular masses are disordered in the layer planes. This property unifies the two most popular smectic phases, marked as A (SmA) - n coincides its layer's normal N; and C (Sc) - n is tilted with respect to N on a tilt angle. Because of this property these phases are considered as two-dimensional liquids. The smectic state is favoured by long aliphatic chains, and amphiphilic interactions (i. e. a trend the aliphatic and polarizable molecular parts to segregate).

A great number of smectic phases also exists, like B, D, E, H .. J. The smectics D, E H, J are called "exotic", but from B to J are genuine crystals that exhibit long-range positional order, but in fact they are three-dimensional stacks of layers weakly attached to each other. For example smectics B are much closer to graphite than to any of the liquid crystalline phases. A remarkable property of smectic structure is that, due to the thermal fluctuations (mainly axial), the smectic state can "wash away". This property restricts the smectic to be realized only in confined space [80].

The characteristic symmetry of the N phase at some conditions (e. g. solution in the nematic liquid of chiral, distinguishing from the its mirror image) breaks out thus leading to an instability in the LC state, the appearance of a "secondary" periodic structure, known as *cholesteric liquid crystal*. Chiral refers to the unique ability to selectively reflect one component of circularly polarized light. Locally, a cholesteric is very similar to the nematic material, they appear to some extent as two subclasses of the same family [80], [85], [88]. The three fundamental liquid crystal molecular structures, nematic, cholesteric, smectic-A and smectic-C are indicated in Figure 2.2.
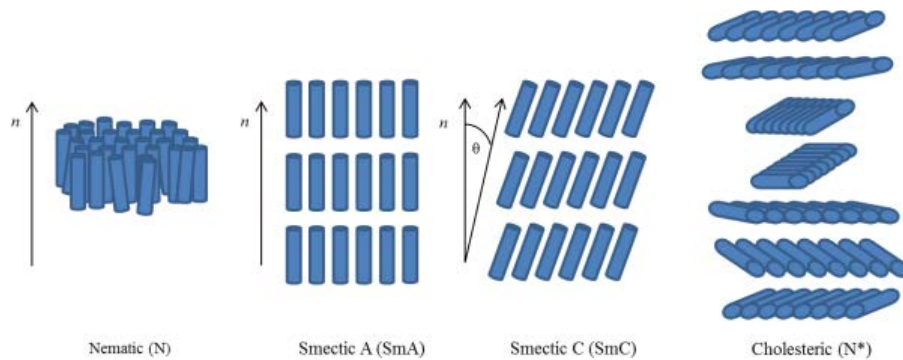

Fig. 2.2. Molecular arrangements of different sub-phase alignments [84].

It should be remarked that the performance of a LC cell/display relies strongly on:

- temperature of smectic-to-nematic transition and of clearing point, determining the so called operating temperature range, for example typical applications with a nematic LC require temperature range between -40 °C and +100 °C;
- elastic constants and (rotational) viscosity, important for the response time and the threshold voltage;
- dielectric anisotropy, determining the behaviour (p or n type) under an electric field, large ε_a decreases the threshold voltage;
- optical anisotropy, determining the optical behaviour;
- threshold voltage, determining the operating voltage range towards low power consumption.

None of the single liquid crystal materials has all the correct physical properties that fulfil the specifications of even the simplest display.

2.3. Active devices

Smart glass, smart windows or switchable glass have voltage dependent optical properties which can be altered by application of specific electrical signals. These technologies include EC, SPD and PDLC devices. Each of these types has different operating principles, advantages and disadvantages.

Smart glass is dynamic, allowing a traditionally static material to become alive and multifunctional. This technology allows for the control of various forms of light including visible light, UV, and IR. Privacy glass products are based on technologies that allow transparent materials (like glass or polycarbonate) to switch, on demand, from clear to shaded or completely opaque (Figure 2.3). The technology can be integrated into windows, partitions and other transparent surfaces in various sectors, including architecture, interior design, automotive, smart retail windows, and consumer electronics [89].

<center>(a)   (b)</center>

Fig. 2.3. (a) - When off, particles are scattered creating opacity for privacy, shading, solar control, or video projection, (b) - when on, particles align, creating transparency for an open atmosphere and natural light [89].

2.3.1 Polymer Dispersed Liquid Crystal device

PDLC consists of micron-sized birefringent liquid crystalline droplets, dispersed uniformly in an optically active and transparent polymer matrix, having spatially varying refractive index and efficient light scattering properties. The light scattering may be switched on by applying an electric field across the film which reorients the molecular directors in nematic droplets to match their ordinary refractive index (η_o) with the refractive index of the polymer (η_lp), thereby, making the film transparent. PDLC films are prepared with the aim to couple the peculiar mechanical properties of a polymeric film (flexibility and high mechanical resistance) and the peculiar electro-optical properties of *LCs* (electrically controllable high optical anisotropy). In PDLCs, confinement of liquid crystals into small cavities dominates over the bulk properties of liquid crystals [90], [91], [92], [93].

The microscopic structural arrangement of PDLCs itself is very complex, but in simplest form it can be sketched as an optically non-absorbing inhomogeneous material composed of an isotropic solid phase (i. e., the polymer), containing almost spherical droplets filled with an anisotropic liquid (i. e., a nematic liquid crystal). In PDLCs, both polymer and liquid crystal have slightly different refractive index values. When no field is applied to the film, director of the nematic droplets has no preferred orientation with respect to the plane of the film. In this case, the difference between refractive indices of polymer and liquid crystal results in the scattering of an incident light. Therefore, film becomes opaque. On the other hand, when electric field is applied to the film it tends to reorient nematic liquid crystal droplets in such a manner that direction becomes parallel to the field (or otherwise, perpendicular to the plane of the film). In this case, ordinary refractive index (η_o) component of liquid crystal matches the refractive index of the polymer (η_lp). Thus, light incident on normal to the film, passes through it without being scattered and film becomes transparent. The operating principal of a common PDLC device is shown in Figure 2.4.
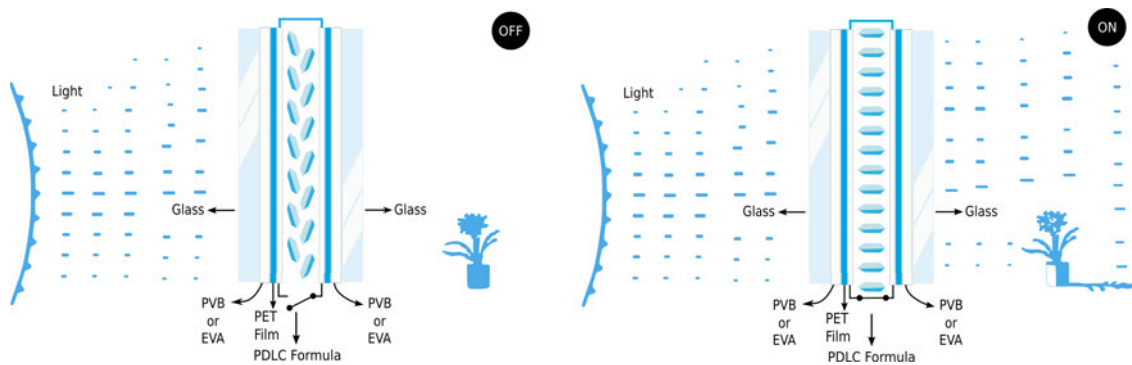

Fig. 2.4. Operating principle of a common PDLC device. From the left side - OFF and ON state [89].

Both, the operating voltage and light scattering properties of PDLCs, depend strongly

on the PDLC film thickness. The droplets shape, size and distribution influence strongly the scattering, reorientation and electro-optical properties of the PDLC films. Haziness effect is minimized by a suitable choice of liquid crystal and polymer constituents with closely matched values of refractive index components [94], [93], [95].

Latest studies on PDLCs, i. e., electric, electro-optic properties [96], [97], [98], [99], reduction of power consumption [100], [101], [102], electro-hydrodynamic effect [103], low power driving techniques [104], [105].

2.3.2 Suspended Particle Device

The development of suspended electrophoretic particle devices has attracted a great attention in the last decades. A SPD device consists of 3-5 layers. The active layer has needle-shaped particles suspended in organic fluid or gel. This layer is laminated or filled between two transparent electrodes. The set of microscopic particles is suspended randomly when no voltage is applied, scattering incident light. If voltage is applied, the particles move their internal charges to a minimum energy state, twisting and aligning as a set, permitting the light crossing through the film. A signal of alternate voltage with different amplitudes can align the particles more or less efficiently (see Figure 2.5), depending on the effective voltage (RMS) of the applied signal [106], [107], [108].

Most recent performance and electro-optic studies on SPD devices are provided here [109], [110], [111], [112], [113].
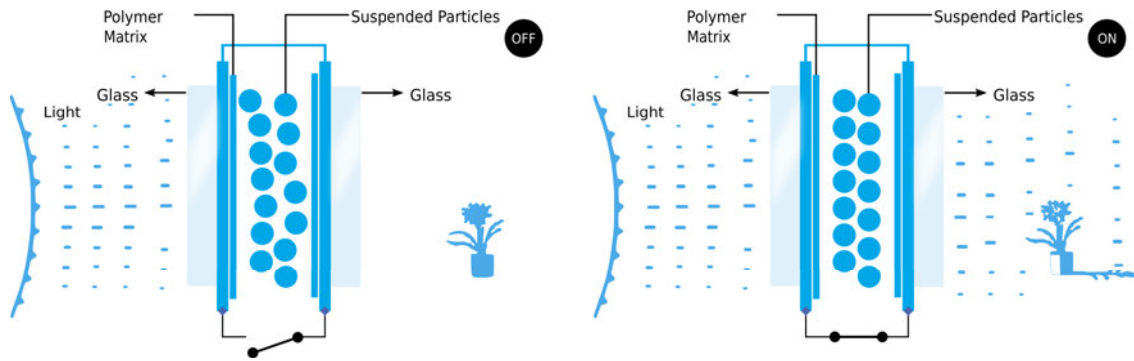
Fig. 2.5. Solid particles alignment with applied electric field [89].

2.3.3 Electrochromic device

Electrochromic glass can be made of either glass or plastic and coated with (physical vapor deposition (PVD) method) multiple thin layers - a separator in the middle, two electrodes on either side of the separator and two transparent electrical contact layers on either side of the electrodes. The basic working principle involves lithium ions, (positively charged lithium atoms — with missing electrons) that migrate back and forth between the two electrodes through the separator. Normally, when the window is transparent, the lithium ions reside in the innermost electrode (on the right side in Figure 2.6, which is

made of, for example, lithium cobalt oxide (LiCoO$_2$). When low voltage is applied to the electrodes, the ions start to migrate through the separator to the outermost electrode (on the left side). Electrochromic layer (dye layer, for example, polycrystalline tungsten oxide (WO$_3$)) starts to change colour based on the amount of current flowing through the layer. Therefore, glass/film starts to reflect the light and effectively turns opaque. Lithium ions remain there all by themselves until the voltage is reversed, causing them to move back so the window turns transparent once again. No power is needed to maintain electrochromic windows in their clear (transparent) or opaque state (light scattering), power is need only to change from one state to the other [114], [115], [116].

Studies on evaluation building energy and daylight performance of electrochromic glazing [117], [118], [119], [120], [121], [122], adaptive glazing systems [123], [124], electro-optic performance [125], [126], [127], [128].
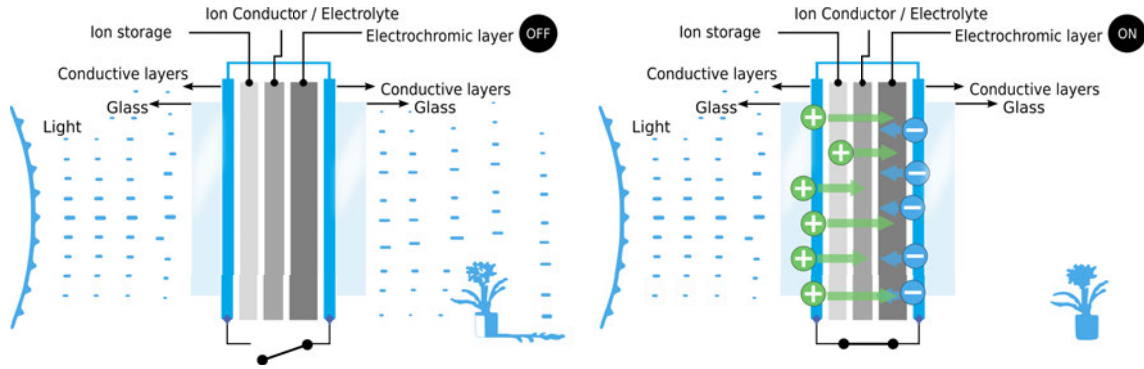
Fig. 2.6. Ion migration into electrochromic layer [89].

2.3.4 *Smectic-A LC* cells

Most LC devices are monostable, with only one possible state in the absence of an electric field. They require a permanent applied voltage and frequent image refreshment, increasing energy consumption. To solve this problem, the use of a bistable display becomes a possibility, where the image (information) is memorized for a long period of time, hence enabling the power consumption to be lowered, similar to electrochromic devices [129].

SmA LC cells offer some important benefits - they can be operated without polarizers, leading to higher light transmittance, improved contrast and remove the need for LC alignment control in manufacturing process. The *SmA LC* is switched between a light transparent state (homeotropic orientation) and an opaque light scattering state (focal-conic texture) by applying an external field with various frequencies (see Figure 2.7). The stability of the optical states in zero electric field comes from a combined effect of the layered structure of the SmA phase and relatively high viscosity of the materials, enabling electro-optic devices energy efficiency [130].
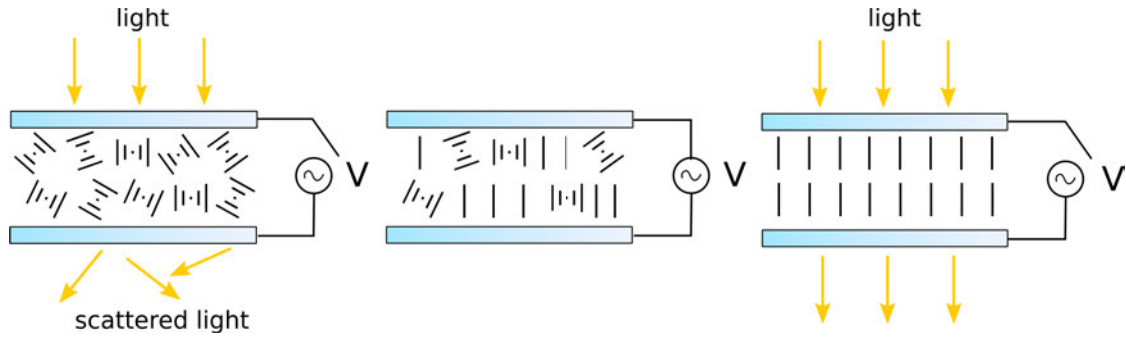
Fig. 2.7. Bistable *SmA LC* cell switching sequence, from the left side - light scattering state (electric field is not applied), LC switching in progress (electric field is applied) and light transmittance state (*LC* cell is fully switched from one state to the other) [131].

Bistable smectic-A *LC* cells have been manufactured by *EuroLCDs Ltd.* (see parameters in Table 2.1). *LCDs* have 300 × 400 mm outer dimensions and active area equally divided into 8 or 25 pixels (see Figure 2.8). *LC* cell pixels can be switched individually or as a single unit if all the pixels are connected in parallel [132], [133] (see Figrue 2.9 for passive matrix driving technique). To maintain a constant cell gap, 15 µm plastic ball spacers with density of 10 pcs/mm^2 have been used. *LCs* have been supplied by Dow Corning Corporation [134, 135].

Table 2.1

SmA LC cell characteristics

Dimensions	300 × 400 mm
Spacer Size	15 µm
Liquid Crystal Type	*Smectic-A*
ITO Resistance	80 Ω/sq
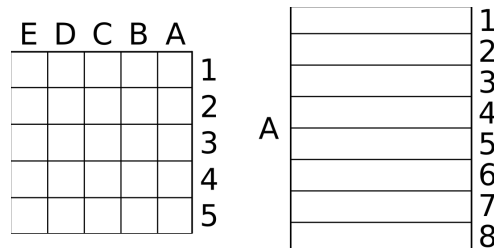
Fig. 2.8. Graphical representation of *LC* cell physical design types. On the left side - 5 × 5 pixel and on the right 8 × 1 design.

Fig. 2.9. Simplified schematic representation of passive matrix driving technique.

2.4. Summary

Brief review of the available LC and active smart glass devices, technologies has been given within the chapter. In total four similar, but at the same time different application products fall into one category - active smart glass devices.

Polymer dispersed liquid crystal device is closest to the SmA LC cell with functionality and obtained electro-optical properties. Biggest differences between both are that PDLC needs constant electrica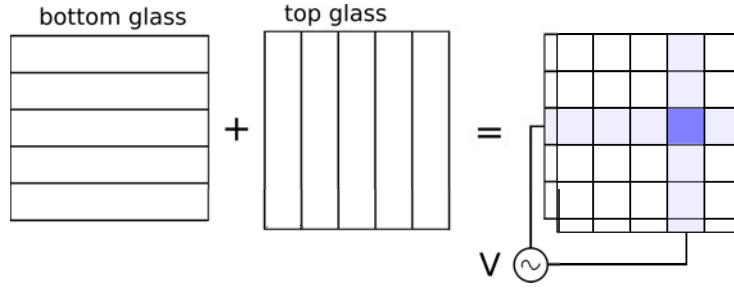l power connection to maintain one of the optical states. Additionally, from reviewed studies above SmA LC cells have better optical properties than PDLC (see Table 2.2). PDLC film appears "milky white" (in light transmitting state) due to the refractive index mismatch encountered by incoming light at the LC/polymer interface.

Suspended particle and electrochromic devices are similar with optical properties, i. e., providing light transmittance from 3-25 % in light scattering state and 60-70 % in light transmitting state. Both devices can be manufactured between two glass sheets and as well as plastic, also colouring options are limited to blue and green. Meaning that both types can be used in smart window applications, as replacement for curtains, blinds, electrical light screens and other appliances used to block direct sun lights. Both devices cannot be used in office or other environments as privacy glass due to the poor optical properties in light scattering state.

From electrical stand point - PDLC and SPD devices are identical, they can be controlled/dimmed to different light scattering levels (light transmittance options) using 65-110 V AC. SmA LC cells require DC balanced 80-240 V signal to switch from state to state. And electrochromic devices require 12 V DC signal to be able to switch to one or other optical state and are the most energy efficient compared to other active smart glass devices.

The biggest advantage of the SmA LC cell is light scattering state - low light transmittance compared to PDLC, SPD, EC devices, blocks everything in the background, any objects and their shapes can not be seen through, in the sunlight cell evenly dissipates the light and brightens up the room without the need for additional lighting to be turned on.

Table 2.2

Smart glass device/cell summary based on studies discussed above

Devices	PDLC	SPD	EC	SmA
Optical properties				
Light scattering state*	3-10 %	3-10 %	10-25 %	2-5 %
Light transmitting state*	<75 %	<70 %	<65 %	<80 %
Colours	clear, bronze, gray, green	blue	blue, green	clear, grey
Electrical properties				
Operating voltage	65-110 V AC	65-110 V AC	12-24 V	80-240 V DC
Switching speed*	100 ms - 5 s	up to 5 s	3-10 min	100 ms - 10 s

* - depends on materials used in production.

In the next chapters *SmA LC* cell operational, electrical properties, as well as functional testing and different defect resolving methods will be provided.

3. OPERATIONAL PROPERTIES

3.1. Objective and tasks

In this chapter SmA LC cell frequency response, electric current measurements will be obtained and reviewed, i. e., important knowledge will be provided about operational principles of SmA LC cells.

In order to meet the objective the following tasks have to be fulfilled:
- Perform frequency response analysis of LC cell;
- Perform voltage measurements on LC cell;
- Perform current measurements and current limiting tests;
- Analyse power consumption of SmA LC cells.

3.2. Frequency response of LC cell

Frequency response is one of the key elements that allows product to be characterized and compared to others. It provides important knowledge about SmA LC switching threshold levels, as well as the most suitable frequencies to reach the highest light transmittance at transparent state and the lowest light transmittance at scattering state. For the frequency response measurements two different design types of SmA LC cells have been manufactured. The main difference was in the dielectric (isolation) coating application procedure: for half of the cells the dielectric coating (Silicon dioxide SiO_2) was applied before ITO ablation process and for other half – dielectric coating was applied after ITO ablation (see Figure 3.1). Contacts were soldered on top and bottom electrodes.
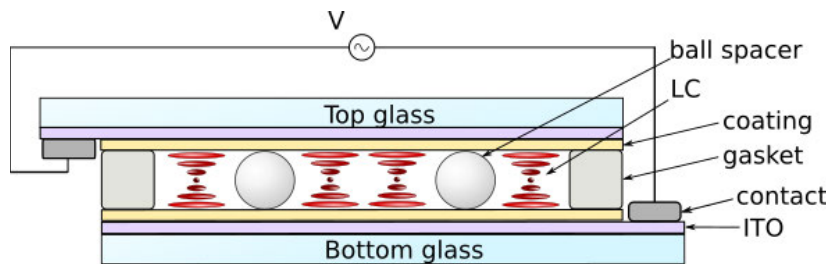
Fig. 3.1. Schematic picture of LC cell: cross–section [136].

Three samples from each design type were used in the experiments (see LC cell parameters here: Chapter 2, section 2.3.4). The reference frequencies – 1 kHz for switching to the transparent state and 50 Hz for switching to the scattering state were chosen on the basis of the LC manufacturer's recommendations [134], [135].

The operating voltage 13 V/µm (195V) was determined in manufacturing process during dielectric boundary tests. Experimental setup, shown in Figures 3.2 and 3.3, consisted of:

1. *SmA LC* cell;
2. optical lenses and white LED light source;
3. optical lenses and photodiode (VTB–1013BH with maximized response through the visible part of the spectrum utilized as light detector);
4. high-voltage wires;
5. low voltage and signal wires;
6. USB communication cable, PC;
7. Optical parameter measurement platform (OPMP), allows the measurements of light transmission and switching speed;
8. alternating high voltage source (AHV), provides necessary voltage level for creating electric field to switch the *SmA LC* cells.
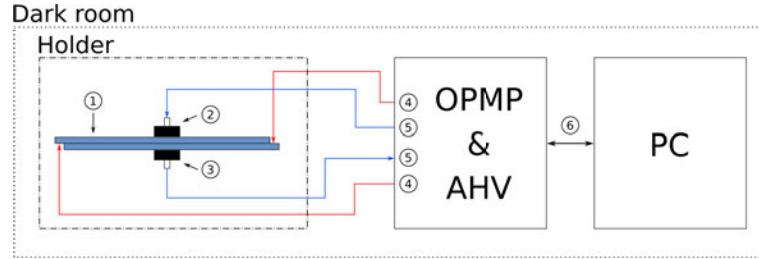
Fig. 3.2. Graphical representation of *SmA LC* cell testing setup.
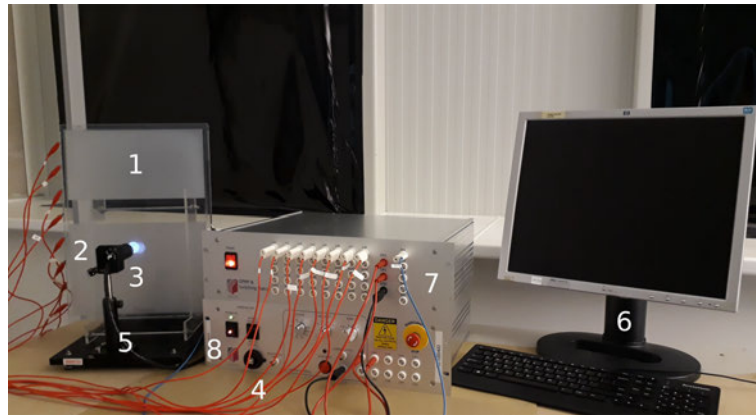
Fig. 3.3. Overview of the experimental setup used for functional testing of *SmA LC* cells.

Obtained *SmA LC* frequency response is shown in Figure 3.4. The light transmittance depends on switching frequency, i. e., *SmA LC* cell is frequency depended, which requires specific Hz and signal waveform to reach certain light transmittance values. In Figure 3.4 the blue curve represents switching from transparent to scattering state and the orange curve – switching from scattering to transparent state.

The frequency range for switching to scattering state is very narrow (10-60 Hz) compared to the frequency range for switching to the transparent state (200-1.5 kHz). *SmA LC* cell could not fully change its state within frequency 5-15 Hz range and above 50 Hz light transmittance starts to increase rapidly. The inner state can be achieved within 60-100 Hz frequency range, i. e., *SmA LC* cell will stay in-between light scattering and transparent state. The peak of the light transmittance (>85 %) for switching to transparent state can be reached only in frequency range between 500 Hz and 1.5 kHz, then it will stay within 85.4-86.1 % range.
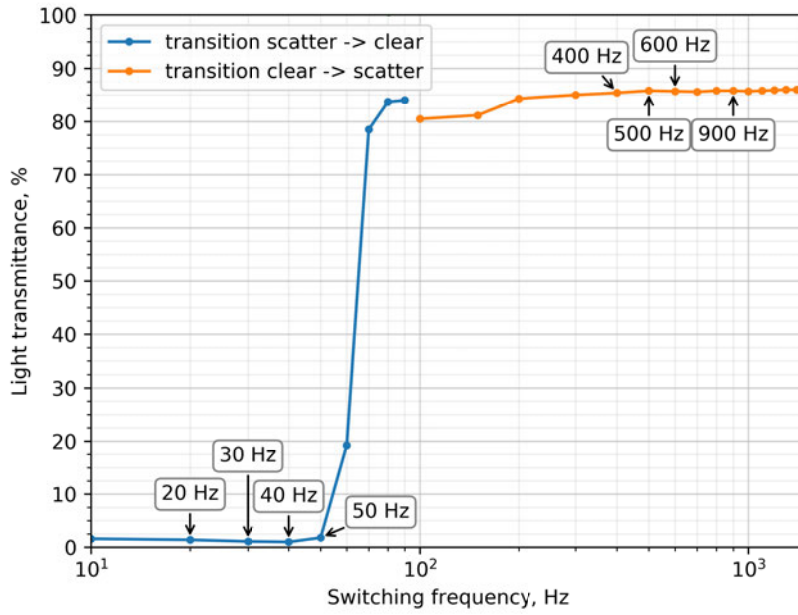
Fig. 3.4. Light transmittance at different switching frequencies.

The more detailed Figure 3.5 shows a close-up of the frequency response for the light scattering state (blue curve) and another important design parameter – switching speed (orange curve). The main focus in this figure is frequency range 10-50 Hz, since 60-100 Hz will set *SmA LC* cell in the inner state. To achieve the highest switching speed (≈1300-1700 ms) and the lowest light transmittance (≈1-1.8 %) in scattering state *SmA LC* should be switched within 20-40 Hz frequency range. The switching speed starts to change rapidly from 20 Hz (≈1300 ms) up to 50 Hz (≈2200 ms). From 70 Hz and up to 100 Hz switching speed does not change. Maximum driving time was set to 5 s and in this period *SmA LC* did not show any signs of leaving the inner state and the light transmittance varied within 20-70 % range. The *SmA LC* cell cannot have both – fast switching speed from state to state and low or high light transmittance – i. e., the driving parameters should be optimized in order to have either responsive switching or good optical properties.
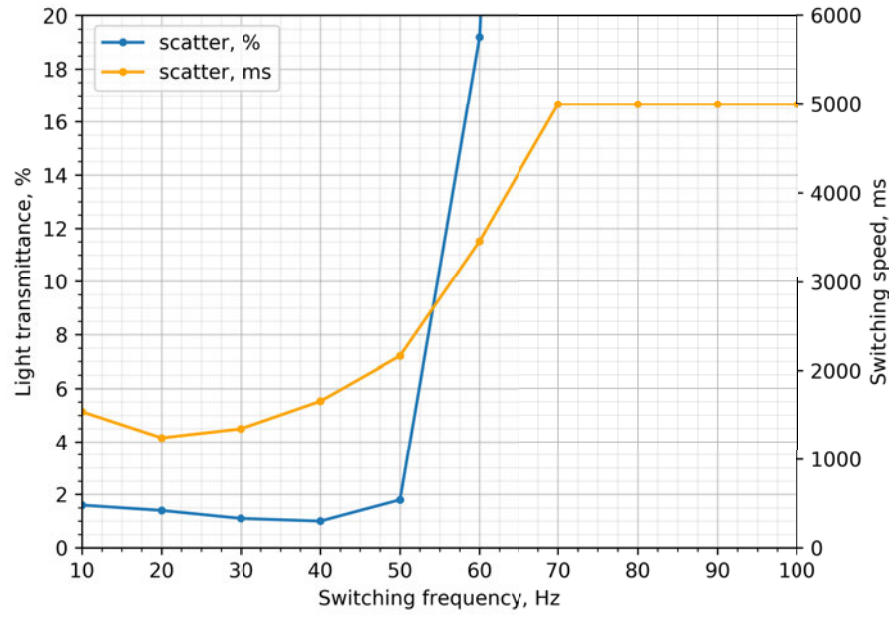
Fig. 3.5. Switching speed (orange) and light transmittance (blue) at different switching frequencies during transition to scattering state.

The second detailed Figure 3.6 shows a close-up of the frequency response for the transparent state. The light transmittance (blue curve) remains relatively constant (>85 %) across the 100-1.5 kHz frequency range. From 100 Hz and up to 250 Hz *SmA LC* cell will stay in the inner state, never fully reaching transmittance or scattering state.

Fig. 3.6. Switching speed (orange) and light transmittance (blue) at different switching frequencies during transition to transparent state.

The switching speed (orange curve) from 100 Hz and up to 500 Hz decreases from ≈400 ms to ≈115 ms, but from 500 Hz up to 1.5 kHz raises linearly up to ≈150 ms. The 400-700 Hz frequency range could be the most suitable for switching *SmA LC* cell to a transparent state, where the light transmittance stays within 85 % and the switching speed varies between 115-150 ms.

3.3.   Electrical parameters of *LC* cell

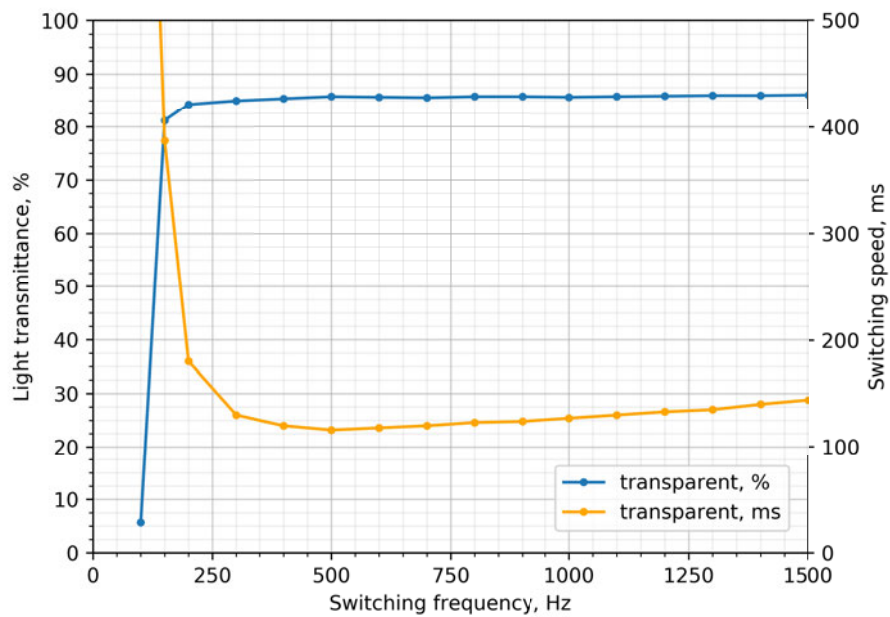Voltage, current and wattage must be clarified in order to electrically characterize the product and compare it to others. The results from the frequency response measurements were analysed and a conclusion was made to update the driving frequencies from scattering state 50 Hz to 30 Hz and transparent state 1 kHz to 600 Hz to obtain better optical parameters and switching response. The updated and the LC manufacturer's recommended driving frequencies were used for voltage and current measurements. The voltage was measured at an output of an AHV source (see Figure 3.7) and on the *SmA LC* cell to verify if cables used for connection and/or *LC* cell will create any voltage drops. Current measurements were done with and without external resistors, i. e., external resistors were used to limit the *SmA LC* cell current. For the current limitation 10 different external metal oxide film resistors with resistances ranging from 8.2 Ohm to 330 Ohm (according to the E24 standard) were used. This allowed to determine the minimum amount of the required current to fully switch the *SmA LC* cell from transparent state to scattering state and vice versa. Voltage and current measurements were done for eight pixels (whole *LC* cell area), six pixels (6/8 area), four pixels (4/8 area), two pixels (2/8 area) and one pixel (1/8 area).
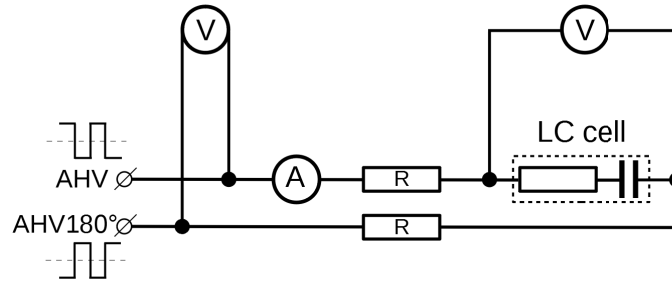
Fig. 3.7. Experimental setup for *SmA LC* cell current limitation and measurements.

The results from voltage and current measurements were analysed, the consumed power (RMS) and watt-hours (Wh) were calculated and they are shown Figure 3.8. The switchable *SmA LC* cell area was adjusted by connecting adjacent pixels in parallel. The power consumption increases exponentially depending on the number of pixels being used. The power consumption reaches the highest point during the transition to a transparent state whilst the whole *SmA LC* cell area is switched. The consumed watt-hour for one switching to the transparent state for a full *LC* cell is ≈0.11 Wh, e. g., for 15 switching

times would be ≈1.65 Wh, compared to an average LED bulb (8.5 W equivalent to 60 W incandescent bulb) ≈0.07 Wh. *SmA LC* cell consumes approximately the same power amount as two 8.5 W LED bulbs.
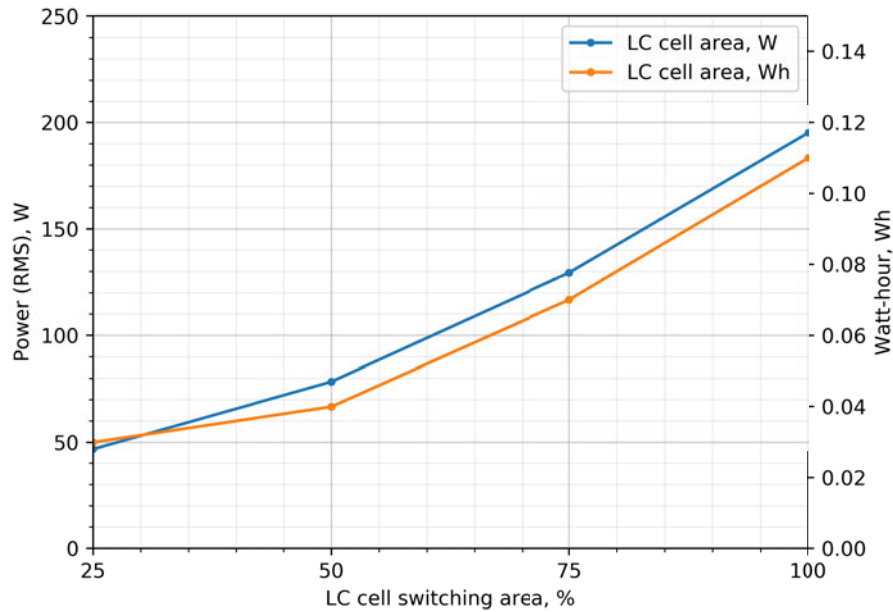
Fig. 3.8. Consumed power (RMS) based on *LC* cell's switching area.

The comparison between 600 Hz and 1 kHz is shown in Table 3.1, for 30 Hz and 50 Hz in Table 3.2.

Table 3.1

Consumed power comparison between 600 Hz and 1 kHz

Driving Frequency	Voltage	Peak Current	RMS Current	Peak Power	RMS Power	Transmittance
600 Hz	190 V	3.12 A	1.03 A	588.21 W	194.42 W	85.10 %
1 kHz	190 V	3.14 A	1.33 A	590.74 W	249.94 W	85.02 %
	Difference:	0.64 %	22.56 %	0.43 %	22.21 %	

Table 3.2

Consumed power comparison between 30 Hz and 50 Hz

Driving Frequency	Voltage	Peak Current	RMS Current	Peak Power	RMS Power	Transmittance
30 Hz	190 V	3.10 A	0.26 A	581.13 W	49.29 W	1.52 %
50 Hz	190 V	3.09 A	0.29 A	579.92 W	55.05 W	1.74 %
	Difference:	0.32 %	10.34 %	0.21 %	10.46 %	

The current measurements with additional current limiting resistors are shown in Figure 3.9. The measurements done for 8 pixels (whole *LC* cell area), four pixels (4/8 area), two pixels (2/8 area) and one pixel (1/8 area). The *SmA LC* cell (8 pixels) require at least 0.9 A of current to switch whole area from scattering to transparent state and obtain >85 % light transmittance. To achieve lower peak current the *LC* cell can be switched sequentially (pixel by pixel or pixel groups), but the switching speed must be taken into account. For example, in order to switch 8 pixels to the scattering state it takes up to 5 s and ≈0.9 A, but if the *LC* cell is switched 4 times by 2 pixels, it will take up to 3-5 s and ≈0.3 A per group switching.
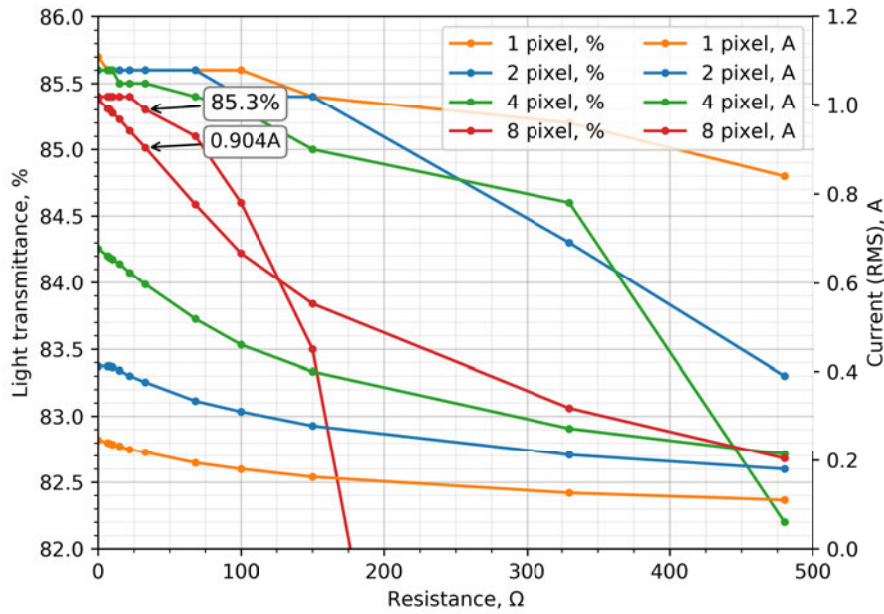
Fig. 3.9. Current measurements with current limiting resistors.

3.4. Summary

Obtained results of frequency response and electrical parameters of the *SmA LC* cell are reviewed and have been given within the chapter.

Frequency response studies show that *SmA LC* cell is functional within 20-50 Hz and 400-1.5 kHz, i. e., if the *SmA LC* cell is being switched with one of the frequencies within the provided ranges it will change its state fully to the light scattering or the transparent state. Obtained light transmittance for the scattering state will be <2 % and for the transparent >85%. The inner state can be achieved within 60-100 Hz frequency range, i. e., *SmA LC* cell will stay in-between light scattering and transmitting state.

In order to choose the appropriate switching frequencies for the *SmA LC* cell, switching speed should be taken in to account, because the switching speed difference between 20 Hz and 50 Hz is ≈900 ms, but for 400 Hz and 1.5 kHz is only ≈285 ms. The *SmA LC* cell cannot have both – fast switching speed from state to state and low or high light

transmittance – i. e., the driving parameters should be optimized in order to have either responsive switching or good optical properties.

The power consumption of $SmA\ LC$ cell increases exponentially depending on the number of pixels being used. The power consumption reaches the highest point during the transition to a transparent state whilst the whole $SmA\ LC$ cell area is being switched. The consumed watt-hour for one switching to the transparent state for a full LC cell is $\approx$0.11 Wh, i. e., $SmA\ LC$ cell consumes approximately the same power amount as two 8.5 W LED bulbs.

The required minimum current amount for 1 pixel is at least 0.18 A and for 8 pixels – 0.9A to switch whole area from the light scattering to the transparent state and obtain >85 % light transmittance.

Next chapter will be devoted to evaluate the behaviour of the $SmA\ LC$ cell in the extended functional testing.

4.   LONG-TERM SWITCHING PROBLEMS

4.1.   Objective and tasks

In this chapter *SmA LC* cells will be tested for extended period of time to identify, review and analyse the most common defects that will appear during and will be detected after the functional testing has been completed.

In order to meet the objective the following tasks have to be fulfilled:
- Analyse *LC* cell:
    - manufacturing processes;
    - testing procedures;
- Create functional testing methodology;
- Perform extended functional testing.

4.2.   Processes and procedures

Every product that has been developed needs to be tested to verify and validate the design and development processes. To make sure the product is safe for customer, complies with necessary product, product group and manufacturing standards, performs the function it is required to perform.

LCDs and *LC* cells go through various stages of testing, e. g., functional, parameter variation testing, Product Development Testing (PDT), Highly Accelerated Life Testing (HALT), Qualification Tests (QT), Failure Oriented Accelerated Testing (FOAT), Burn In Test (BIT) [137], [138], [139]. All of the testing methodologies have been thoroughly analysed and improved by some manufacturers and research laboratories. These testing stages are adaptive, i. e., same testing principles could be used for other products as well, to obtain the best results each of the stages should be modified to the specific product needs. However, there are no better or worse, each testing methodology play crucial role in products quality, performance, maintenance etc.

After assembly process *SmA LC* cells go through the first electrical testing, where LC breakdown boundaries are clarified, see Figure 4.1. It is necessary to determine the *LC* cell maximum operating voltage, so that a system that operates with this type of *LC* cell in normal operational and fault conditions would never reach this critical boundary.

When the *LC* cell breakdown thresholds are acknowledged, operational properties must be determined (both – clear, scatter frequencies and operating voltage) [140] in order to obtain the highest light transmittance in a transparent state and the lowest in a scatter state. Switching speeds and power consumption must not be forgotten, because end device should be energy efficient and responsive, see Figure 4.2.
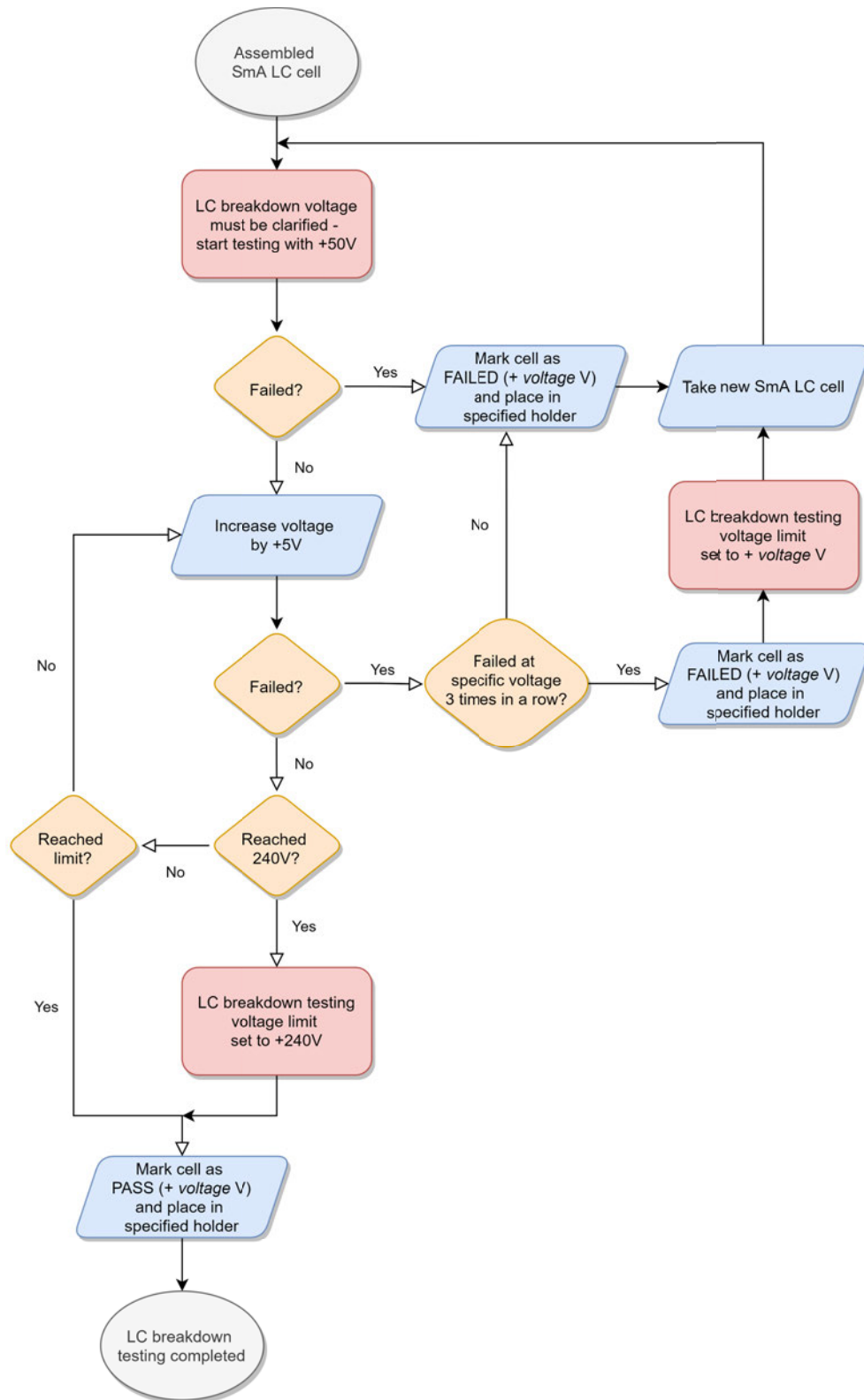
Fig. 4.1. *SmA LC* cell first electrical testing (LC breakdown) diagram.
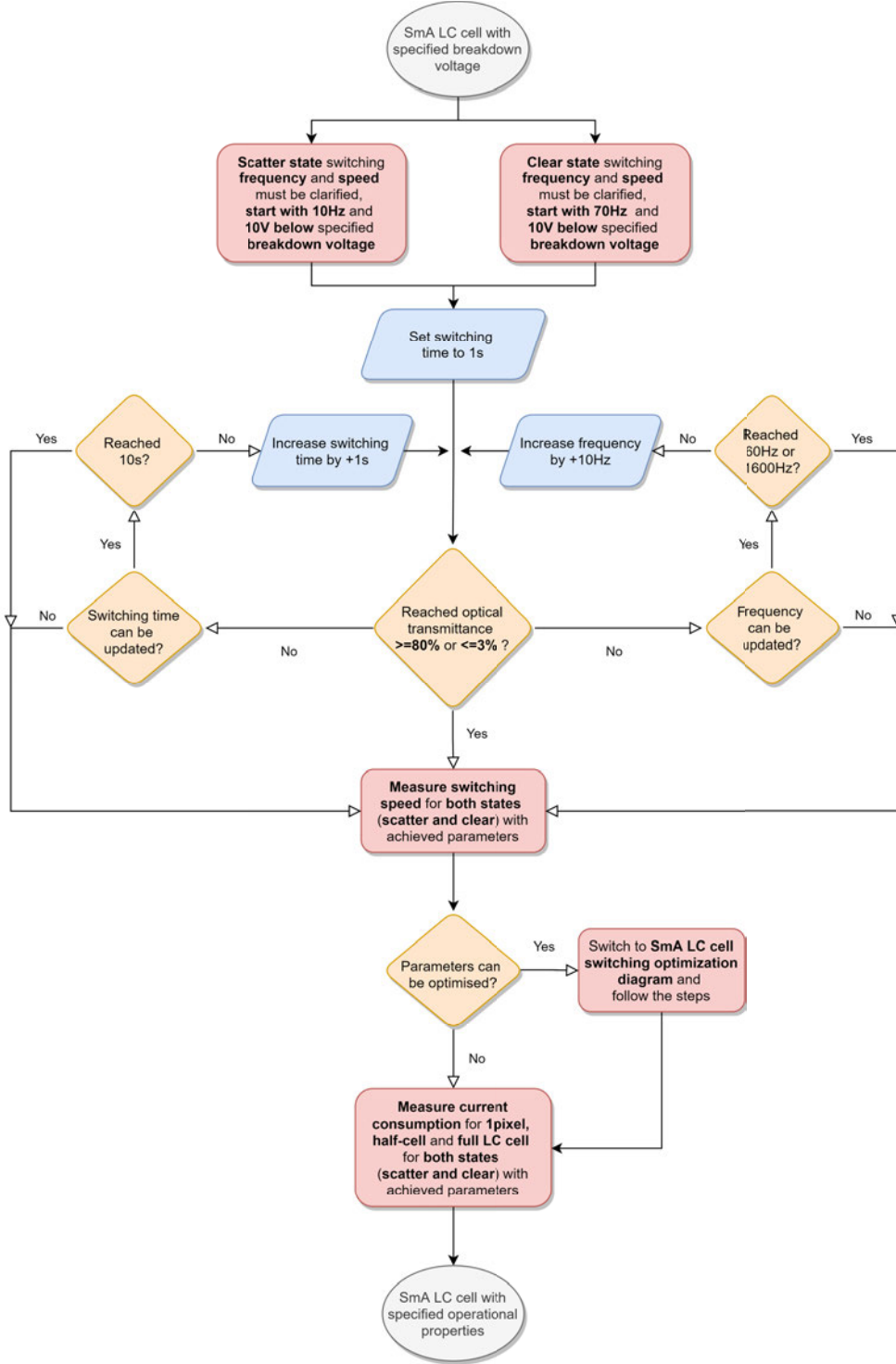
Fig. 4.2. *SmA LC* cell operational parameters determination diagram.

4.3. Functional testing procedure

All the *SmA LC* cells were tested with the same parameters (see Table 4.1) and one full functional testing cycle consists of:

1. Switching to the scatter state and the operational parameter measurement;
2. Pause between state-state switching;

3. Switching to the transparent state and the operational parameter measurement;
4. Pause between state-state switching;
5. Pause between switching cycles.

SmA LC cell functional testing parameters

Measurement frequency	500 Hz
Measurement time	4 s
Measurement angle	0 °
Switching voltage	13 V/µ (195 V)
Switching waveform	DC balanced square wave
Scatter state frequency	30 Hz
Transparent state frequency	600 Hz
Switching time (scatter)	3 s
Switching time (transparent)	1.5 s
Pause between state-state	2 s
Pause between cycles	5 min

Each one was switched at least 1000x (full cycles), that took around 40 hours to complete. Together were tested 20 *LC* cells over more than 30 day period of time. Every 100+ cycles the measurements were stopped and the *LC* cells were photographed to see if any visual changes occurred.

LCDs and *LC* cells are functionally tested in different environments, one of which is the dark room. In such a room it is possible to minimize the error in the optical transmittance measurements due to the constant lightning. But it is not always possible to provide a constant room temperature unless a climate chamber is used where it can be set to constant value. Climate chambers are used to make sure that the developed product will be able to function completely at different extreme humidity and temperature levels. These tests are carried out to obtain maximum functionality limits so that the user knows in what type of environment the product can be used without damaging it. In this case, the temperature was dependent on the settings of the building's ventilation system. In Table 4.2 environmental parameters are listed.

Table 4.2

The environment in which the experiments were conducted

Premises	dark room
Lighting	constant
Temperature	room temperature

The experimental setup used for extended functional testing was the same as the one mentioned in the Chapter 3, section 3.2.

4.4. The ideal *SmA LC* cell

SmA LC cell that has been switched at least 1000 times and more, visually should look like one in the Figure 4.3. Where the light transmittance in a transparent state is >85 %, active area is clear of anything other than the view in background of the *LC* cell. The view through this *LC* cell should be equal or very close to the view of the 2-to-3 chamber polyvinyl chloride (PVC) window. The scatter state should block everything in the background, any objects and their shapes should not be seen through. Scattered area should look even, without any blank spots, unswitched corners, wavy, etc. In the sunlight area must be an eye-pleasing and should evenly dissipate the light.

(a)

(b)

(c)
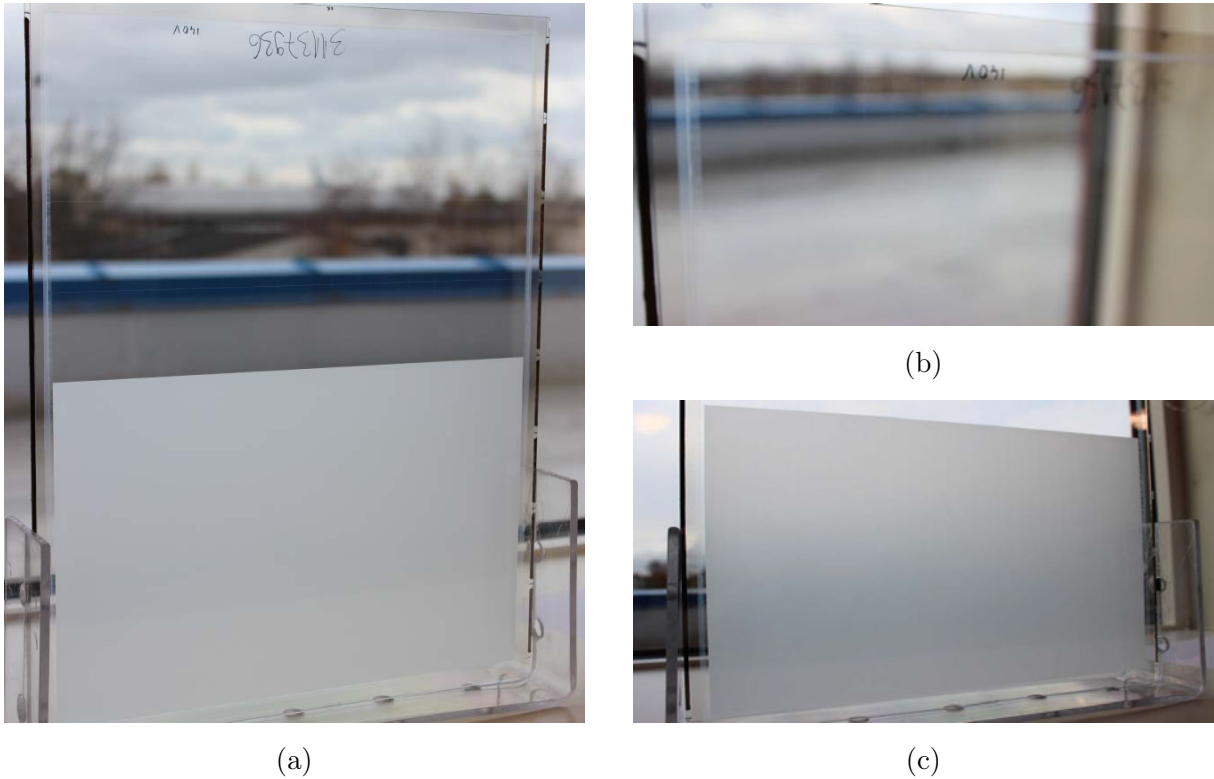
Fig. 4.3. Full scale 300×400 mm *SmA LC* cell, where the active area is divided (switched to the opposite states) into the transparent (upper side) and the scatter (lower side of the *LC* cell) states.

4.5. Obtained defects

The figures below show the most common defects that appeared during and were detected after extended period of functional testing. In Figure 4.4 *SmA LC* cell with 5×5 design were tested. To be more precise - only one pixel (C3) was switched 1000+ times from state to state and pixels around it were observed to understand the impact on them. Before the testing was started - initial pixel states were set, i. e., pixel C2 and C3 was switched to the transparent and pixel C4 to the scatter state.

After the functional testing pixel C2 remained still in transparent state. Near the pixels' perimeter, parts of the active area have changed to scatter state, i. e., near laser ablation lines (pixel separation lines) area unevenly changed from transparent to scatter state. Additionally random LC clusters (from distance visually looked like dots) are randomly switched to scatter state, C2 pixel looks dotted.

Pixel C3 transmittance has decreased by ≈ 0.4 % and not completely changed its state to transparent at the end of extended period of functional testing. C3 perimeter, just like C2, has unevenly changed from transparent to scatter state. The centre of the pixel C3 looks visually smooth, even and there are no noticeable LC clusters.

In Figure 4.4 pixel C4 is partially visible, but its initial state has not changed, i. e., still in light scattering state. By looking closely at the figure, it is possible to see that near laser ablation lines pixel has unevenly started to change to transparent state. Simirarly to C2 pixels' C4 area near ablation line LC clusters have randomly switched to transparent state.
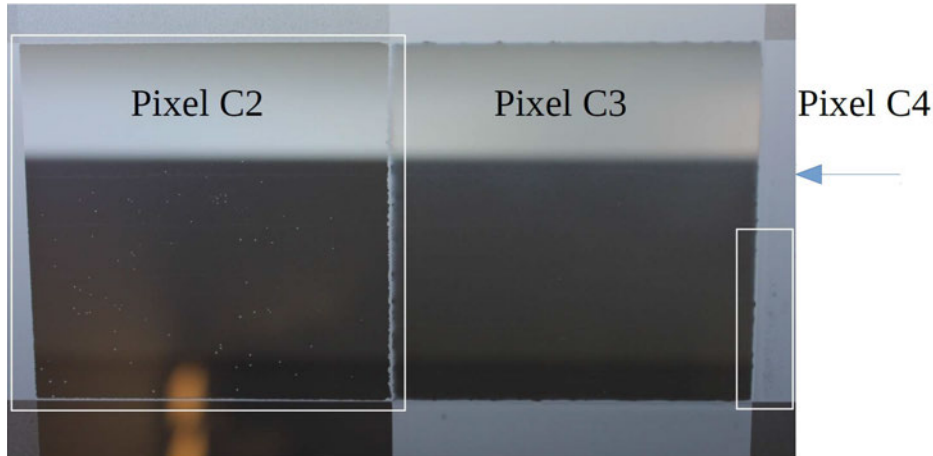
Fig. 4.4. *SmA LC* cell (5×5 design) close-up of the three middle pixels - C2, C3 and C4.

The figures 4.5 (a) and (b) are close-up of Figure 4.4 pixel C3 captured with the microscope. In these Figures 4.5 it can be seen that LC cluster zones around the C3 perimeter are not completely switched to transparent state. Pixels C2 and C4 were not grounded during the functionality testing of pixel C3. From obtained results, it can be concluded that the electrical field impacts pixel that is next to the pixel that is being switched from state to state. Also LC tends to get stuck near the pixels perimeter (cannot

change its state completely) and with time (if pixel switching routine does not change) small LC clusters tend to get bigger and start to form larger un-switched areas.

(a)   (b)
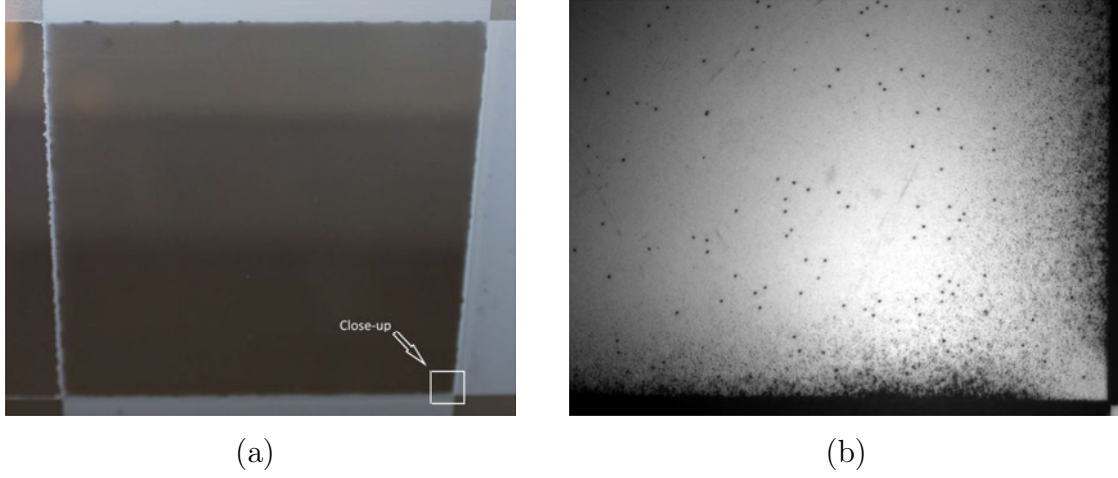
Fig. 4.5. *SmA LC* cell (5 × 5 design): (a) - close-up of the middle pixel C3 and (b) - close-up of the lower right corner of pixels C3 captured with microscope.

The second common defect that appeared was brighter laser ablation lines, compared to the rest of the *LC* cell area or pixel it self. This defect was especially evident in the *SmA LC* cell 8 × 1 design. In Figure 4.6.(a) it can be seen that pixel laser ablation lines are brighter than rest of the pixels' area and pixels' outline looks wavy, the edges are visually rugged. The rest of pixels' area is uniform, no random LC clusters, etc.

In Figure 4.6.(b) laser ablation lines are more pronounced, i. e., they are more scattered (with lower light transmittance) then rest of the *SmA LC* cells' area. *LC* cell has not completely changed its state to scatter, all of the active area is wavy and not uniform. Near laser ablation lines both type of the LC clusters can be observed, i. e., bigger and smaller LC clusters that are changed to transparent and scatter states.

(a)   (b)
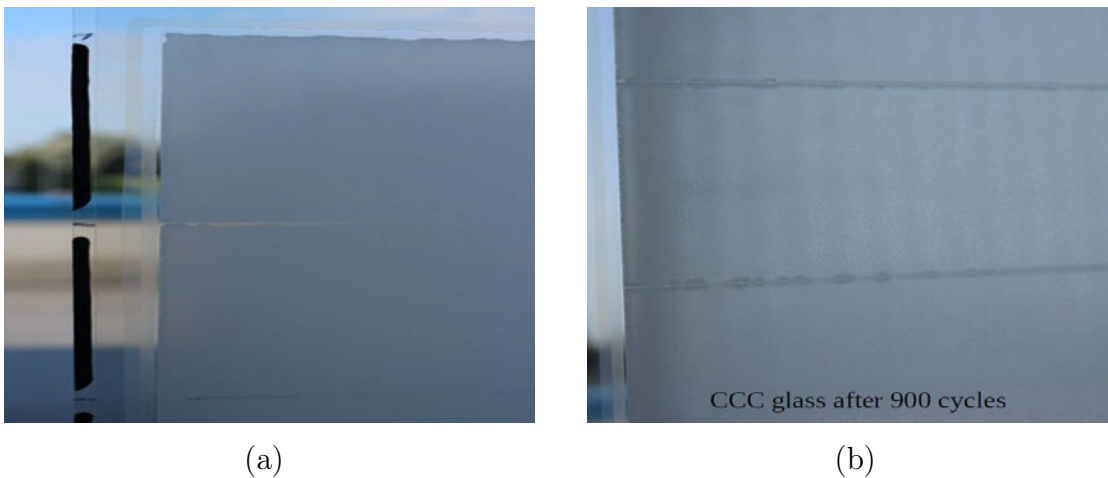
Fig. 4.6. *SmA LC* cell (8 × 1 design): (a) - close-up of pixels laser ablation lines and outline, (b) - close-up of pixels active areas and laser ablation lines.

The less common defect is shown in Figures 4.7:(a-c), *LC* cells' active area was not uniform. Some parts of the active area have completely changed their states, others stuck in inner state. These parts could not completely change to either (transparent or scatter) state. In Figure 4.7.(c) *SmA LC* cell transparent state has two more pronounced areas that have not completely changed their state. Same thing can be observed in the scatter state (see Figure 4.7.(b)).

(a)

(b)

(c)
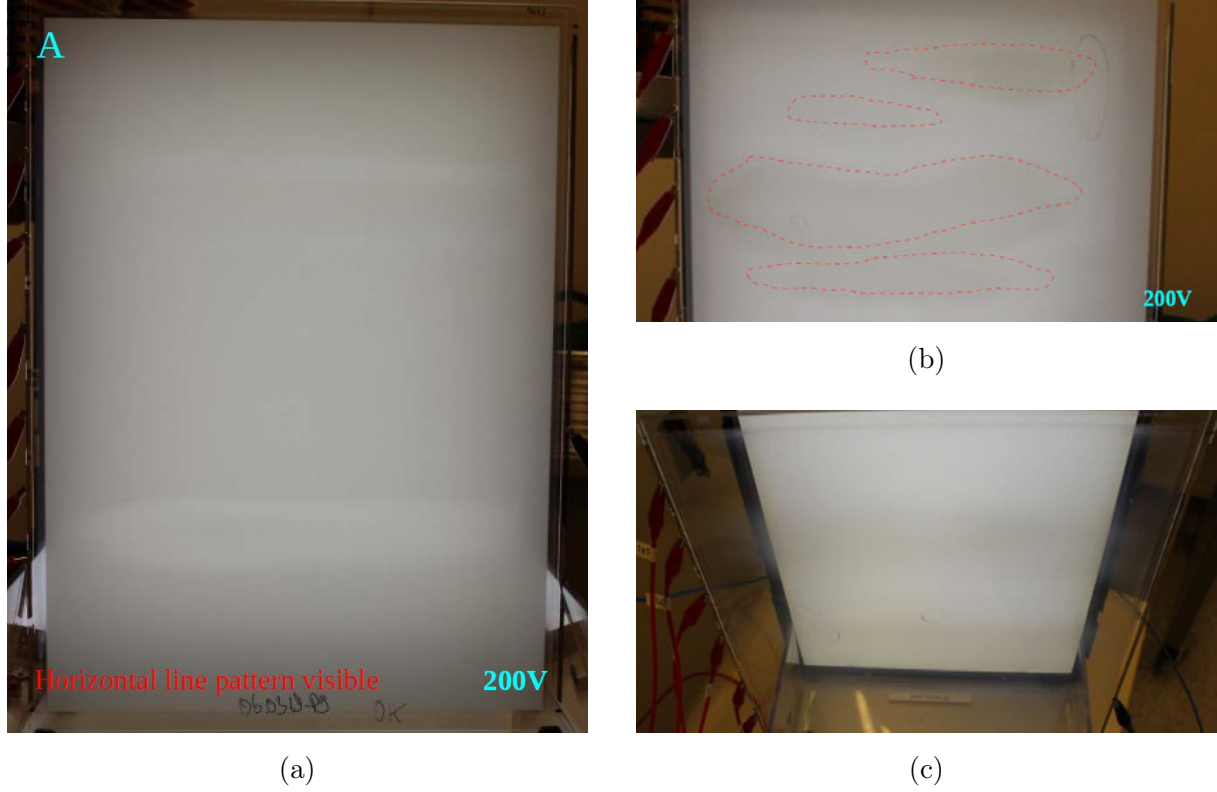
Fig. 4.7. *SmA LC* cell (8×1 design): (a) - close-up of the scatter state, (b & c) - close-up of the transparent state. Additional background (behind the *LC* cell) lightning was used for better visual defect identification.

4.6. Summary

Extended functionality testing methodology and experimentally obtained defects (most common) that appeared during and were detected after testing has been given and reviewed within the chapter.

SmA LC cells with 8×1 design tend to have more pronounced laser ablation lines, i. e., *LC*, near these lines, with time will have better optical properties – lower light transmittance compared to the rest of pixels' active area. Also pixels edges tend to be more rugged then straight line.

Only few of the tested *LC* cells had non uniform active area, some with wavy pattern. Visually sharp light scattering differences, LC did not completely change its state, stuck in the inner state (LC clusters with different light transmittance values near each other).

In both states (transparent and scatter) these regions could not be completely switched to either state.

5×5 design or similar chess patterned layouts will have problems with switching sequence, image or text displaying. LC tends to create zones, clusters near laser ablation lines. Pixels that are next to the pixel that is being switched, will start to randomly change their state and create random LC clusters.

SmA LC cells are sensitive to the switching parameters, due to the low parallel resistance [141], they tend to warm up with intensive switching from state to state. Switching speed rises and LC cell stays within the inner state. This should be taken in account when switching sequence is being developed, additional pause between state to state switching must be included. SmA LC cells will never often and quickly change their states without specified pause in-between switching steps - only in cases where testing procedure requires to understand LC degradation boundaries.

Next chapter will be devoted to understand different switching pattern and parameter impact on LC cell.

5. DEFECT RESOLVING

5.1. Objective and tasks

In this chapter defect resolving methods will be proposed and switching waveform optimization performed to further improve overall functionality and visual looks of *SmA LC* cells.

In order to meet the objective the following tasks have to be fulfilled:

- Analyse the impact on *LC* cell by:
    - testing cycle sequence;
    - switching parameter optimization;
- Perform different switching waveform tests;
- Perform and analyse other defect resolving methods.

5.2. Testing cycle and parameter optimization

Without extended research it is impossible to optimize the switching parameters for *SmA LC* cells, therefore three different experimental series were performed. The first experiment was devoted to understand if testing cycle and parameter optimization could resolve different defects that were described in Chapter 4, section 4.3 and prevent their appearance in long term. All *SmA LC* cells were tested with the same parameters (Chapter 4, section 4.3).

The Figure 5.1 below shows one of the most common defects, i. e., random LC cluster zones in the middle of the pixels' active area. When LC molecules are in the lowest energy state and weak electric field is applied LC molecules due to the low rotational force start to create random LC clusters. Uneven thickness of the *SmA LC* cell, inappropriate switching parameters or testing cycle could be the reasons why the defect occurred.
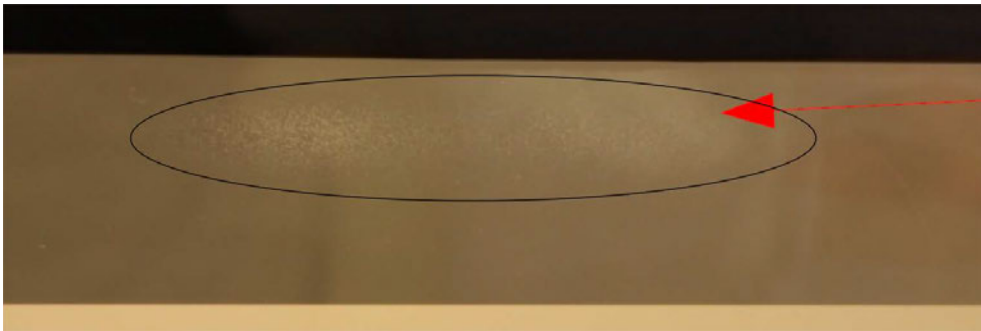
Fig. 5.1. Unswitchable (stuck) LC cluster zones in inner state before testing cycle and parameter optimization.

In this case, to eliminate and fix this defect, it is necessary to optimize the driving voltages and update the testing cycle sequence. Additional pauses should be added between pixel-pixel and state-state switching. Also different switching voltages should be used for each switching state. Obtained results are shown in Figure 5.2 and parameter comparison in Table 5.1

Updated functional testing cycle consists of:

1. Switching to the scatter state and the operational parameter measurement;
2. Pause between pixel-pixel switching;
3. Pause between state-state switching;
4. Switching to the transparent state and the operational parameter measurement;
5. Pause between pixel-pixel switching;
6. Pause between state-state switching;
7. Pause between switching cycles.

Table 5.1

SmA LC cell optimized and non-optimized switching parameter comparison

	Before	After
Measurement frequency	500 Hz	
Measurement time	4 s	
Measurement angle	0 °	
Switching voltage (scatter)	13 V/µ (195 V)	
Switching voltage (transparent)	13 V/µ (195 V)	9 V/µ (135 V)
Switching waveform	DC balanced square wave	
Scatter state frequency	30 Hz	
Transparent state frequency	600 Hz	
Switching time (scatter)	3 s	7.5 s
Switching time (transparent)	1.5 s	
Pause between pixel-pixel	0 s	1 s
Pause between state-state	2 s	5 s
Pause between cycles	5 min	

Recommendations would be to start with the switching time and then with pause extension optimization. If switching time and pause extension does not work, additional pauses in between pixel-pixel switching and state-state must be added. Switching voltage optimization must be used as the last option, because it will require to change the switching timings and pauses once again, see Figure 5.3.

Fig. 5.2. Unswitchable (stuck) LC cluster zones disappeared after testing cycle and parameter optimization.

Fig. 5.3. *SmA LC* cell switching optimization diagram.

With switching parameter and testing cycle optimization it is possible to improve different type defect visual conditions, e. g., pixels wavy outline and rugged edges. These defects tend to return after X number of cycles, but are less pronounced (see Figure 5.4). The needs of end user experience and finished product visual look must be taken into

account, e. g., if *SmA LC* cell is mounted into 2-to-3 chamber PVC window, then the available active area will reduced by ∼2-5 % with black isolation material and pixels wavy outline, rugged edges will not be visible.
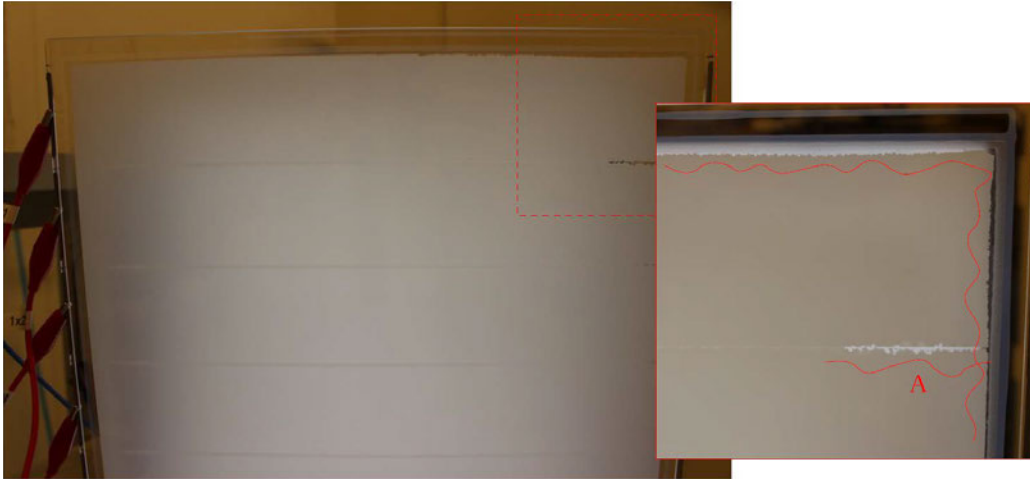
Fig. 5.4. Defected *SmA LC* cell - pixels with wavy outline, rugged edges and unfixable separation line between two pixels.

Near laser ablation lines (pixel separation lines) unevenly changed area from transparent to scatter state can only be partially improved, non of the experiments, testing methods and optimizations showed any potentials to completely eliminate this problem. With the naked eye it is practically impossible to see this defect in transparent sate, but in scatter state with special attention to the lines defect can be noticed.

Similar result was obtained for uneven (discoloured) active area and was partially improved. Defect is related to the production of the display and the methods used there. Manufacturing processes must be optimized to avoid such a defect (see Figure 5.5).
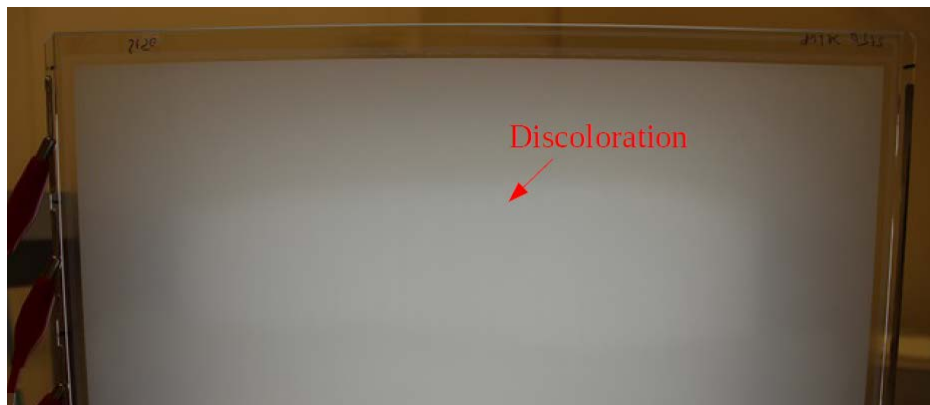
Fig. 5.5. Discoloured pixels active area of *SmA LC* cell in light scattering state. Additional background (behind the *LC* cell) lightning was used for better visual defect identification.

5.3. Switching waveform optimization

The second experiment was carried out to verify if different switching waveforms could improve switching from pixel-pixel and state-state, i. e., prevent or eliminate different defect appearance.

In order to realize such an experiment additional equipment was needed, because AHV (alternating high voltage source) used in previous experiment could generate only DC balanced square wave signal with different amplitudes and timing periods. High voltage power supplies, signal generator, operational amplifier and other equipment can be seen in Figure 5.6, but simplified functional schematic in Figure 5.7.
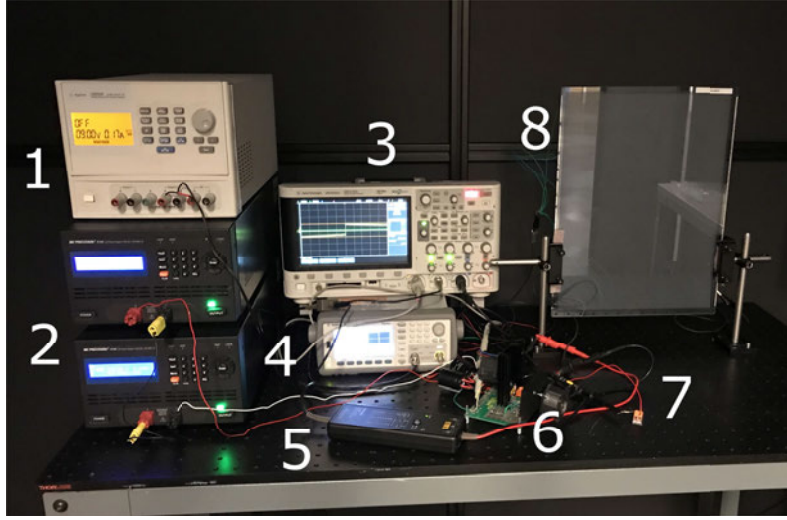
Fig. 5.6. Overview of the experimental setup used for switching waveform optimization for *SmA LC* cells. Used equipment: 1 – Agilent U8032A, 2 – B&K Precision 9184, 3 – Agilent DSOX2014A, 4 – Agilent 33500B, 5 – Tektronix P5200, 6 – Apex PA93, 7 - Rx (current measurement resistor), 8 – SmA LC cell.
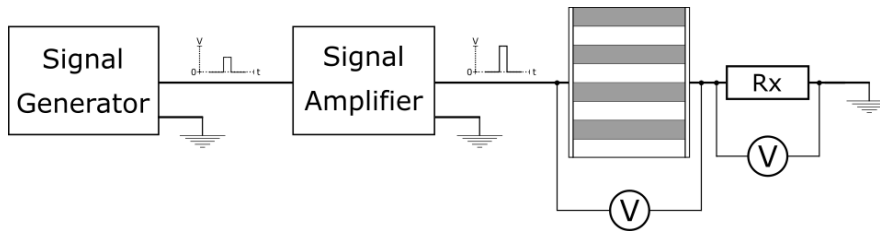
Fig. 5.7. Simplified functional schematic of electrical parameter measurement setup, where waveform generator generates sine wave, sawtooth or other custom signal, signal amplifier amplifies switching signal from 100 V up to ± 200 V and outputs it to *SmA LC* cell and additional Rx resistance.

Different switching waveform experiment were held to understand if with other type of waveforms better optical parameters or higher switching speeds would be achievable. To properly switch $SmA\ LC$ cell from state-state the switching signal must be DC balanced, therefore, sine and triangle signal waveform generation, amplification was tested.

Multiple units were tested with three different switching signals, but the switching voltages, pauses between pixel-pixel and state-state, switching timings, etc. remained unchanged. Obtained results are quite interesting, see Tables 5.2 and 5.3, because units could change their states with DC balanced square and sine wave signals, but with triangle $SmA\ LC$ cell stuck in the inner state and stayed there.

Sine wave results are similar to square wave, but with improvements in electrical parameters, i. e., less current, power is required to switch the $SmA\ LC$ cell, meaning - lower energy consumption and lower maintenance costs in long term use case. The downside are worse optical parameters, in transparent state light transmittance decreased by $\approx$4-8 %, but in scatter state increased by $\approx$6-10 %.

Table 5.2

Switching waveform experiment - transparent state

Signal	RMS, A	Peak, W	RMS, W	Energy, Wh	Close
Square	0.11-0.12	198-207	22-23	0.25-0.26	1.3-1.4
Sine	0.14-0.16	135-157	29-32	0.09-0.15	7.5-11.2
Triangle	N/A	N/A	N/A	N/A	N/A

Table 5.3

Switching waveform experiment - scatter state

Signal	RMS, A	Peak, W	RMS, W	Energy, Wh	Close
Square	0.23-0.25	287-306	46-48	0.18-0.26	85.3-85.6
Sine	0.07-0.08	135-157	13-15	0.05-0.06	10.5-14.4
Triangle	N/A	N/A	N/A	N/A	N/A

5.4.   Other defect resolving methods

The third experiment was carried out to understand if temperature treatment in pre-heated industrial oven would "reset" or remove defects that appeared during extended functional testing or with inappropriate switching cycle and/or testing parameters, see Figure 5.8.

Fig. 5.8. Unswitchable (stuck) LC cluster before temperature treatment. Darker, brighter and transparent spots resemble inhomogeneities of polyimide coating.

Different switching parameter and testing cycle sequence optimization was done, but without any useful results. In this case *SmA LC* cell was put into preheated oven at 100 °C. LC melted within first 25 minutes, then left in room temperature to cool down, since melted *SmA LC* looks exactly the same as cooled down it is hard to tell how long it took to cool down ($\approx$2-3 h) (see Figure 5.9).

After *SmA LC* cell was fully cooled down to room temperature scattering state was visually checked. *LC* cell looked homogenous again without any defects visible to naked eye. To verify if *SmA LC* cell is working properly and defects does not appear again, unit was tested for 100+ cycles with the same switching parameters and testing cycle sequence.

Since this unit was placed in an insulated window package and filled with argon, the only defect that had occurred after heating treatment was the curvature of the outer glass sheets. The visual appearance of the active area was smooth, ablation lines very fine, practically invisible. Functionally switched from state-state and from pixel-pixel without any problems.

<div align="center">(a)   (b)</div>
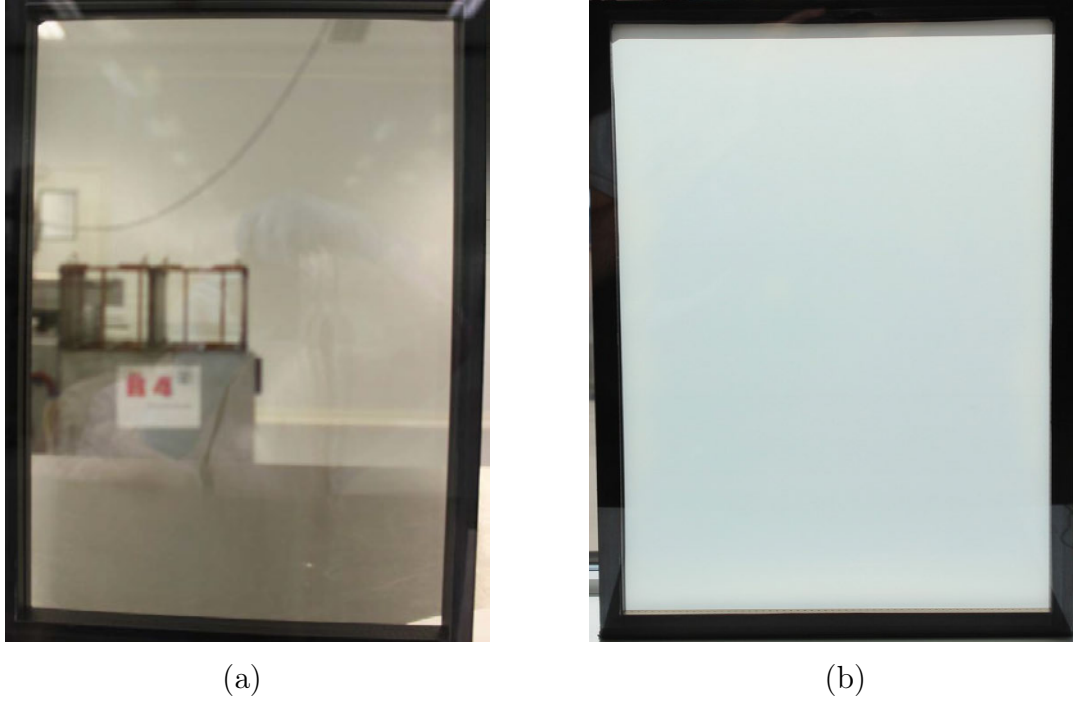
Fig. 5.9. *SmA LC* cell after temperature treatment: (a) - *LC* cell looks clear due to the LCs high viscosity (viscosity changes based on LCs temperature), (b) - *LC* cell after 100+ testing cycles, no visual and functional defects were found.

5.5. Summary

SmA LC cell switching parameter, testing cycle optimization, different switching waveform and other defect resolving methods have been given and reviewed within the chapter.

All kinds of optimizations are good until (ideally) functional peak of the product is reached, i. e., in our case - the best optical properties, the highest light transmittance in the transparent and the lowest in the scatter state. But not always it is possible to achieve both states at their best due to the need for different switching voltages, switching sequence or switching/pause time optimization. The more product is optimized the more complicated electronics design will become, resulting in higher final product costs.

Not always it will be possible to optimize all parameters, i. e. by obtaining lower light transmittance in the scatter state, switching to the transparent state may be difficult. It may be necessary to extend the switching time or increase the voltage, but this can and will most likely affect the scatter condition again. There will be trade-off between visual performance and functional switching time.

The use of different driving signals showed that it is possible to switch these *SmA LC* cells quite well. Sine wave can be used in different cases where there is no need for (compared to square wave) fast switching *LC* cells, but with an emphasis on optical parameters as well as power consumption in the long run. It is possible to create a custom

signal shape that would improve the switching speed, obtain the same optical parameters, reduce power consumption, but definitely complicate the design of electronics.

Temperature treatment proved that it is possible to "restart" the SmA LC cell after being damaged with incorrect switching parameters, testing sequence or other unknown source. This method should be used only if defect could not be fixed with switching optimization. Procedure should be tested and verified with defected LC cells to understand if other type of defects could also be fixed.

Next chapter will be devoted to understand and create equivalent load model for electronics simulation software.

6.   ELECTRICAL SIMULATION MODEL

6.1.   Objective and tasks

In this chapter *SmA LC* cell electrical properties will be experimentally obtained and the electrical model for electronics simulation software will be introduced.

In order to meet the objective the following tasks have to be fulfilled:

- Literature review about *LC/LCD* cell/device characterisation and electrical simulation model creation;
- Perform *SmA LC*:
    - cell ITO resistance measurements;
    - capacitance measurements.

6.2.   *ITO* layer and dielectric resistance

The need of a good simulation model for an *LC* cell or *LCD* becomes apparent during the design of driving system. LC capacitance is critical in the simulation of *LC* cell or *LCD* pixels and is voltage dependent due to the LC characteristics.

Simple parallel RC circuits usually represent the behaviour of *LC* cell or *LCD* in a variety of situations. These electric circuits are of great practical interest, since they can be used in countless applications ranging from theoretical studies to simulations of *LC* cell or *LCD* elements [142].

Due to the anisotropy of LC material, the LC capacitance (C_{LC}) is not constant. It varies from a minimum capacitance when no voltage is applied across the *LC* cell to a maximum capacitance when the *LC* cell is fully turned on [143]. Thus, the LC capacitance (C_{LC}) is bias and time dependent. This mechanism has been thoroughly analysed by some LC manufacturers and laboratories. However, the formulation is very dependent on the specific LC type [143], [144].

One particular feature of *SmA LC*s is a marked hysteresis in their switching to the extent that dielectric re-orientation (or other disturbances of the smectic structure) does not relax when the electric field is removed, dielectrically re-oriented *SmA LC*s remain in the switched state until further forces are applied [134], [145], [132]. This is explained via reference of the nature of the processes, which are used to switch such LCs [146], [135].

The *LC* cell can be considered as an ideal capacitor. Due to its construction, it is very similar to a flat capacitor, where both plates are made up of two ITO layers and between them there is LC material with ε_r [147]. More precisely is to take into account conductivity loss and *LC* cell approximation in a narrow band with a non-ideal capacitor model (Figure 6.1), where R is the electrical resistance of the output (ITO layer and dielectric) and C is the electrical capacity of a flat capacitor.

By adding additional R and C elements, a model describing the *LC* cell up to a frequency range of 10^{-1}-10^7 Hz can be obtained [142].
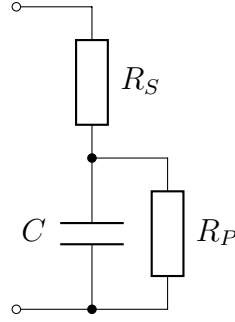

Fig. 6.1. *LC* cell equivalent electrical circuit

The first experiment has been devoted to obtain R_S that mainly consists of conducting, transparent layer, ITO resistance measured in ohms per square (Ω/sq). Typical values are 40–100 Ω/sq. The thicker ITO layer, the lower resistance and optical transmittance and vice versa. To achieve high optical transmittance and good conductivity, ITO resistance must be chosen between 80–100 Ω/sq.

Additionally, ITO layer must be patterned to reduce LC breakdown. ITO must be patterned in strips such that the resistance of the strips would increase, thus lowering the current in the series. The great benefit of using patterned electrode is that the overall resistance of the cell does not change, and the capacitive charging times of the cell are not affected. Unfortunately, the patterning is visible to the eye since it scatters light. Compromise between the optical quality and electrical properties should be found [133], [140], [136].

The experimental setup was the same as the one mentioned in the Chapter 5, section 5.3. Equivalent series resistance R_S (Equation 6.1.) can be determined by rapidly applying voltage and measuring the voltage on a series-connected resistor (R_x = 5-10 Ω) (Figure 6.3). At the first moment of time C is a short circuit and voltage divider is formed. R_S can be calculated as follows:

$$R_S = \frac{(V_s - V_x)R_x}{V_x} \tag{6.1.}$$

The obtained results from the measurements of equivalent series resistance R_S are shown in Figure 6.2. Two different R_x values were used (5.2 Ω, 10.4 Ω). The measurements were made at a number of V_s values ranging from 5 V to 195 V with 5 V increment step. Blue dots represent R_x = 5.2 Ω and orange dots - R_x = 10.4 Ω. The green line represents the mean value of both R_x value measurement data.

Pronounced deviation is noticeable in 5 V to 30 V range. When the *LC* cell is energized, switching is gradually taking place. This is due to the low rotational force caused by the electric field applied to liquid crystal molecules if they are in the

lowest energy state. From 40 V to 195 V R_S does not depend on the applied voltage and $R_S \approx 71\ \Omega$.
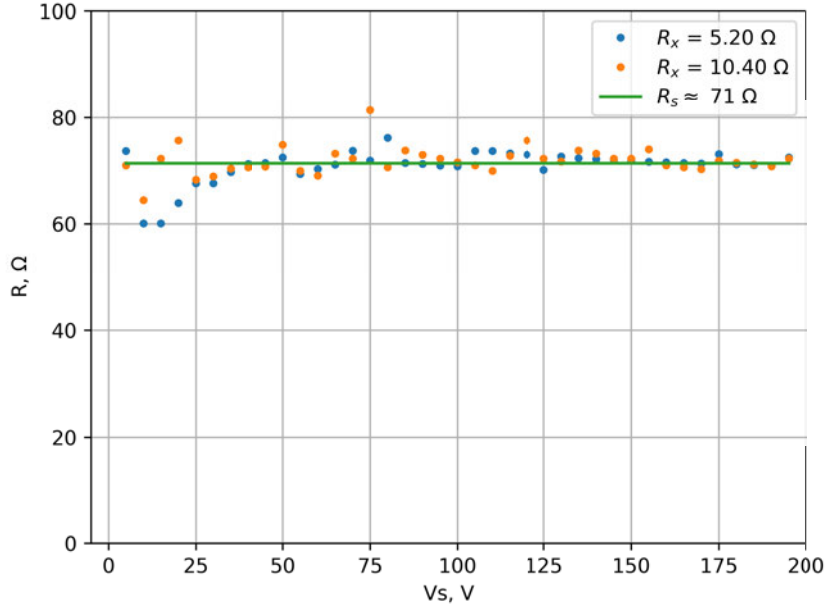
Fig. 6.2. Equivalent series resistance R_S dependence of V_S.
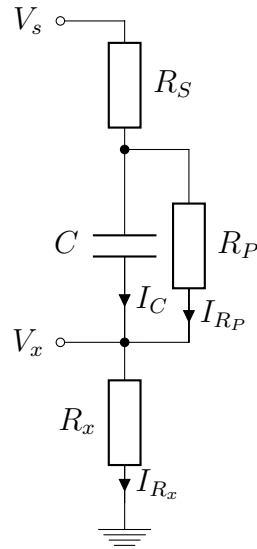
Fig. 6.3. Simplified electrical parameter measurement circuit

6.3. *LC* capacitance

An effect related to reorientation experienced by the LC molecules is change of capacitance offered by a single LC pixel, C_{LC}. Due to the dielectric anisotropy of LC mixture, this capacitance is voltage dependent [147].

In the second experiment equivalent parallel resistance R_P and capacitance C were determined. In this case V_s was not a rapid voltage step but more gradual and $R_x = 1k\ \Omega$ (Equation 6.2.) [136]:

$$\frac{V_x(t)}{R_x} = I_{R_x}(t) = I_C(t) + I_{R_P}(t).$$

(6.2.)

After certain amount of time C is fully charged, $I_C = 0\ and\ I_{R_x} = I_{R_P}$. Since $R_S \ll R_x,\ R_P$, then R_P can be calculated according to the voltage divider formula (Equation 6.1.). When R_P is found I_C can be calculated as follows:

$$I_C(t) = I_{R_x}(t) = I_{R_x}(t) - I_{R_P}(t) = \frac{V_x(t)}{R_x} - \frac{V_s - V_x(t)}{R_P}$$

(6.3.)

Total charge accumulated on the capacitor can be obtained by integrating $I_C(t)$:

$$Q_C = \int I_C(t)dt$$

(6.4.)

Fully charged equivalent capacitor capacity can be calculated as follows:

$$C = \frac{Q_C}{V_s - V_x}$$

(6.5.)

Measured $SmA\ LC$ cell C capacitance change over V_S are shown in Figure 6.4. Dotted blue line represent C and orange line the mean value of C in LC cells' functional range 100-195 V. Obtained capacitance from 5-40 V ≈44 nF with a slight drop at 35 V. Then, increasing the V_s, the capacitance increases up to 100 V and ≈53 nF. With the voltage being continuously increased capacitance change within 10 % range. LC material dielectric permeability depends on the position of molecules and can be influenced by the external electric field. Capacitance dependence of the applied electric field is not linear.
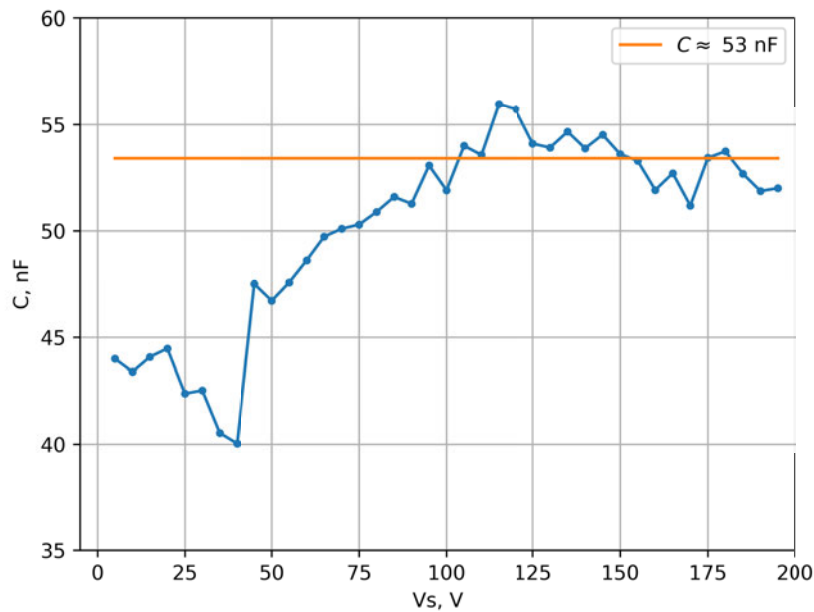
Fig. 6.4. LC cell capacitance C dependence of V_S.

6.4. *LC* resistance

An LC with high viscosity needs high intensity electric field for operation, but in this case an LC electrical breakdown is likely to occur. Electrical breakdown in the cell is observed when the electric field intensity E in the LC layer is above a specific breakdown value E_{br}. The E_{br} is governed by the conductivity of the LC, surface smoothness of the electrodes, defects in coatings as well as point defects, such as dust particles, in the LC layer. The dielectric breakdown in an *LC* cell is a complicated process discussed elsewhere [148]. Based on the parameters of the equivalent electrical circuit, it is possible to calculate power dissipation on R_S and R_P:

$$P_{R_S}(t) = I_x^2(t) * R_S = R_S * \frac{V_x^2(t)}{R_x^2} \tag{6.6.}$$

$$P_{R_P}(t) = \frac{U_c^2(t)}{Rp} = \frac{(V_s(t) - V_x(t) * (1 + \frac{R_S}{R_x}))^2}{R_P} \tag{6.7.}$$

The obtained results of equivalent parallel resistance R_P are shown in Figure 6.5. Dotted blue line represents measured R_P and orange line the calculated mean value of R_P in *SmA LC* cell functional range 100-195 V. From 5 V and up to 20 V there is an increase in resistance as it should be with different LC materials (example Cholesteric LC) were R_P increase up to 1 MΩ. In this case rapid decrease follows and parallel resistance decreases to ≈13.5 kΩ and from 125-195 V stays within 5 % deviation. The low resistance is explained by the difference of the LC composition itself.
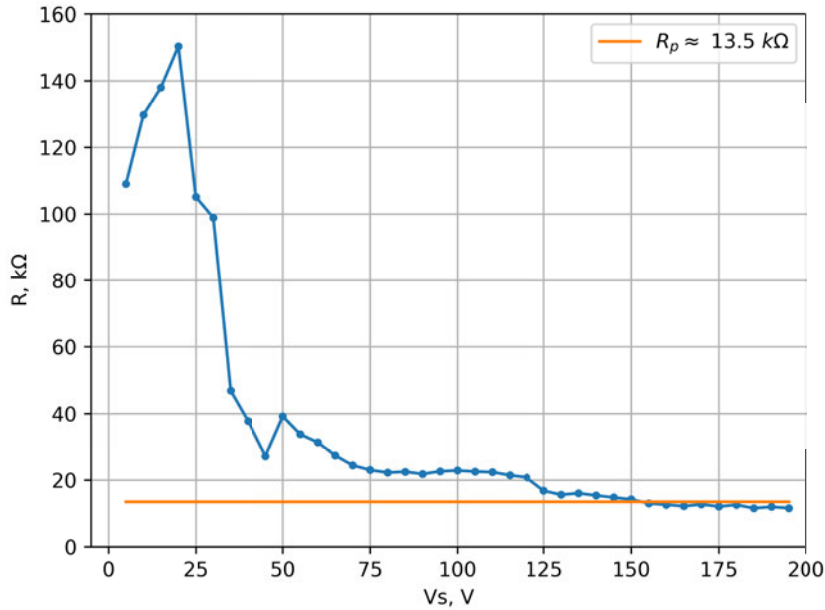
Fig. 6.5. Equivalent parallel resistance R_P dependence of V_S.

Obtained power dissipation results on R_S and R_P are shown in Figure 6.6. Dotted orange line represents R_P and blue – R_S resistance. At 195 V V_S, which is the typical operational voltage of *SmA LC* cells, $R_S \approx$2.1 W and $R_P \approx$6.3 W. Both the equivalent parallel and series resistance shows exponential growth. Most of the power is dissipated on R_P. R_P can be reduced by minimizing V_S voltage; however, this would affect the *LC* cell switching speeds and optical parameters. R_S cannot be reduced due to the proportional current required by the *LC* cell to charge its equivalent capacity.
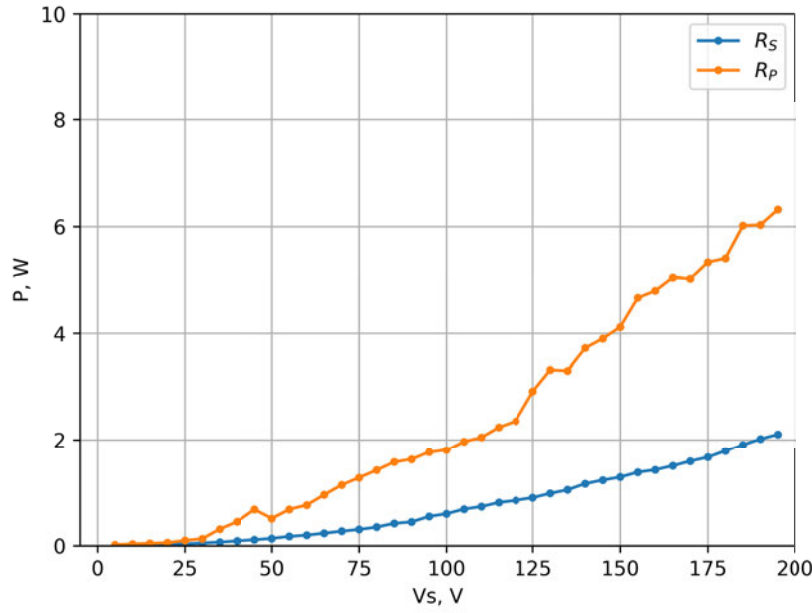
Fig. 6.6. R_S and R_P power dissipation dependence of V_S.

6.5.   Summary

The experimentally obtained *SmA LC* cell equivalent series, parallel resistance and capacity have been given within the chapter.

Obtained results of series R_S and parallel resistance R_P show that R̲S̲ ̲s̲t̲a̲y̲s̲ ̲w̲i̲t̲h̲i̲n̲ p̲r̲o̲v̲i̲d̲e̲d̲ ̲I̲T̲O̲ ̲t̲o̲l̲e̲r̲a̲n̲c̲e̲s̲ ̲(̲±̲2̲0̲ ̲%̲)̲ and do not depend on the applied voltage. R_P resistance is lower compared to other *LC* cell parallel resistance, e. g., cholesteric *LC* cell. Great attention should be paid to the power dissipation, with such a low internal parallel resistance LC can quickly reach its temperature limit and *SmA LC* cell will stop working.

Capacitance C measurements provide information about *SmA LC* cells' functional range 100-195 V, at which the applied electric field is high enough to be able to rotate LC molecules and change LC state from transparent to scattering and vice versa. Additional in-depth research should be done in 5-95 V range to fully understand LC molecule threshold voltage at which they start to rotate.

Simulation model parameters $R_S = 71 \ \Omega$, $R_P = 13 \ k\Omega$, $C = 53 \ nF$ will provide sufficient

information about electric functionality of large size 300×400 mm SmA LC cell and can be integrated into the development of larger systems.

Experimental testing methodology can be adjusted to other LC cell types and used to understand their behaviour and obtain both equivalent series and parallel resistances, as well as capacitance in order to create new simulation models.

Next chapter will be devoted to summarize the products, equipment and upgrades that have been created during the research of the doctoral thesis.

7. PRODUCTS, HARDWARE, UPGRADE

7.1. Objective and tasks

In this chapter the *SmA LC* product summary will be introduced, as well as the new and the existing equipment upgrade overview.

In order to meet the objective the following tasks have to be fulfilled:

- Review of *SmA LC* products;
- Overview of custom built hardware;
- Overview of existing equipment upgrade.

7.2. *SmA LC* products

In order to find a functional application for the *SmA LC*, cells with different ITO patterns were designed and manufactured during the research of the doctoral thesis. Most of the time 8×1 and 5×5 *LC* cell designs were used in the experiments, because the produced samples were functionally stable and the measurement standard deviation was very low. 8×1 design was created to visually and functionally replicate blinds & shades in a modern way and could be fitted into the standard window frame.

Since *EuroLCDs Ltd.* are capable of producing samples only up to 300×400mm in size, the logical solution for one of the products was a standard window frame with four of these cells, see Figure 7.1.

Fig. 7.1. *EuroLCDs Ltd.* presented *SmA LC* smart glass window in Kurzemes Demo Center.

The product was developed together with the help of ICT (information and communication technology) Ventspils city funding project and placed for demonstration in the Kurzemes Demo Center [149], [150], as well as presented at the Ventspils High Technology Park (VATP) exhibition [151].

Such an 8×1 design 4-cell standard window can also be used as a projection screen (see Figure 7.2.a), where one or more cells are switched to the light scattering state and the projector displays information, e. g., the product information, office hours or any other useful information. Accordingly, there is no need to advertise in another format outside the building, and this information can be instantly changed to current and does not require any additional material costs. The visually projected image is clear, with high resolution and good contrast.

In addition, 2×2 cell samples have been created for small presentations (see Figure 7.2.b), i. e., easily portable samples to demonstrate their functionality. Also, these samples can be used as small placards on which the image is projected by small portable projector, or these cells can be integrated into the doors as a transparent window that can be closed (switched to the light scattering state) to create a sense of privacy.
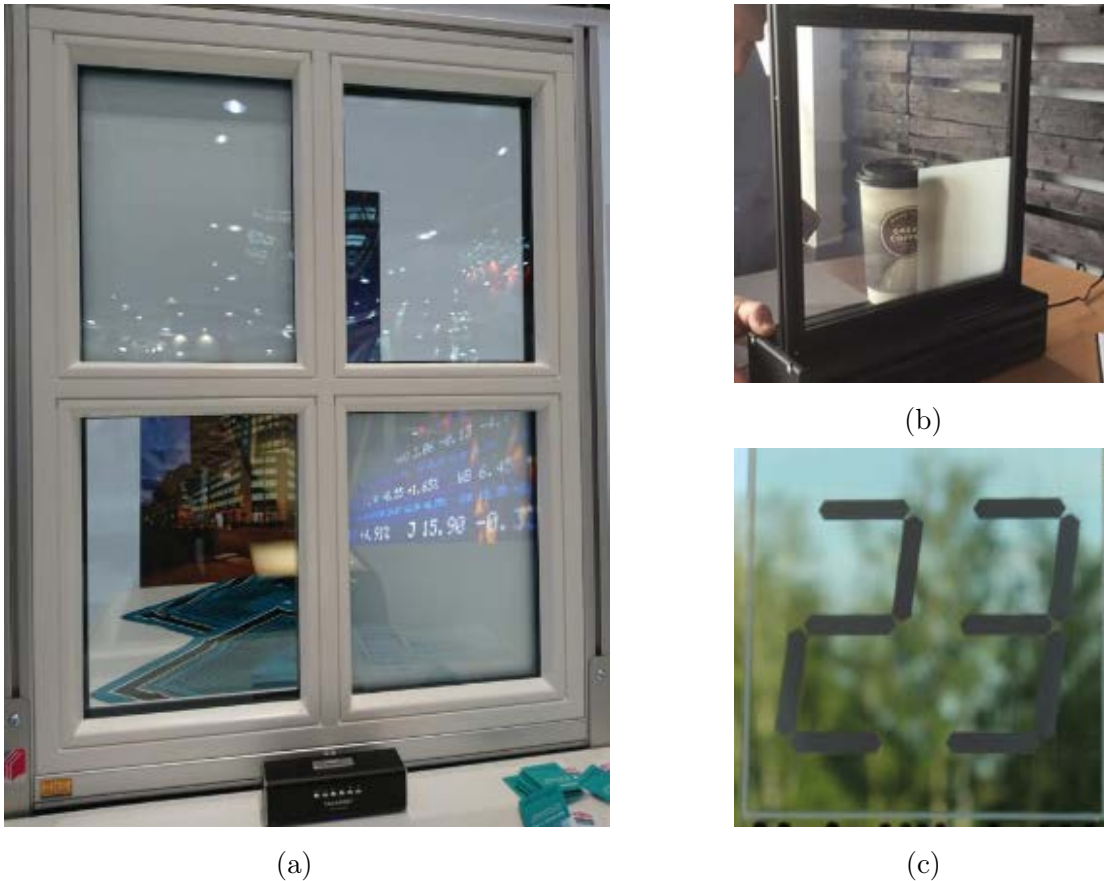

(a)   (b)

(c)

Fig. 7.2. *SmA LC* cell products: (a) - 4-cell standard window, (b) - 2x2 design for presentations, (c) - numeric design *LC* cell [152].

The *SmA LC* cell design with one of the biggest potential could be a numeric cell (see Figure 7.2.c), i. e., cell that can display numeric values from 0-9. Such a design can be used as a separate speed sign on the highway, with additional light-reflecting coating or material at the back of *LC* cell for higher contrast and visibility. It is possible to change the speed limit if an accident has occurred or road repairs are taking place and it is necessary to slow down the traffic in order not to create additional risks on the highway.

The most technically difficult *SmA LC* product was a high-resolution cell, where the size of one pixel was 1x1mm. Such a project was implemented together with company called Lumotune, which further glued four identical cells together and created one large smart information sign/stand, see Figure 7.3.

Such a demo product perfectly proves that *SmA LC* cells can be used both as informative signs, as well as a light-transmitting or diffusing devices, and a stylish accessory, e. g., cell could be used as modern painting on the wall that changes the image after certain amount of time and would never be the same.

(a) (b)

Fig. 7.3. Lumotune smart glass demonstration: (a) - paintings: from the left side Mona Lisa and The Scream, (b) - example of advert [153], [154].

7.3.   Custom built hardware

7.3.1   Measurement platform

One of the most important devices that has been created is an OPMP (Optical Parameter Measurement Platform), which allows optically and electrically verify the *SmA LC* manufactured samples. The functional block diagram can be seen in Figure 7.4 and finished device in enclosure in Figure 7.6.

The OPMP is able to perform electrical and optical measurements automatically, i. e. using "recipes" (pre-saved settings) for different product variations, to test up to five *SmA LC* cells (identical design) at the same time. It is possible to optically measure

light transmission, viewing angle and switching speeds from state-state. By connecting an external AHV, it is possible to electrically verify pixels (of different designs) - all simultaneously, sequentially, alternately, etc. The OPMP has custom built software (see Figure 7.5), that allows to perform measurements remotely, saves all measurements in .csv and .png formats, all measurement curves, switching speeds, calibration data, etc.
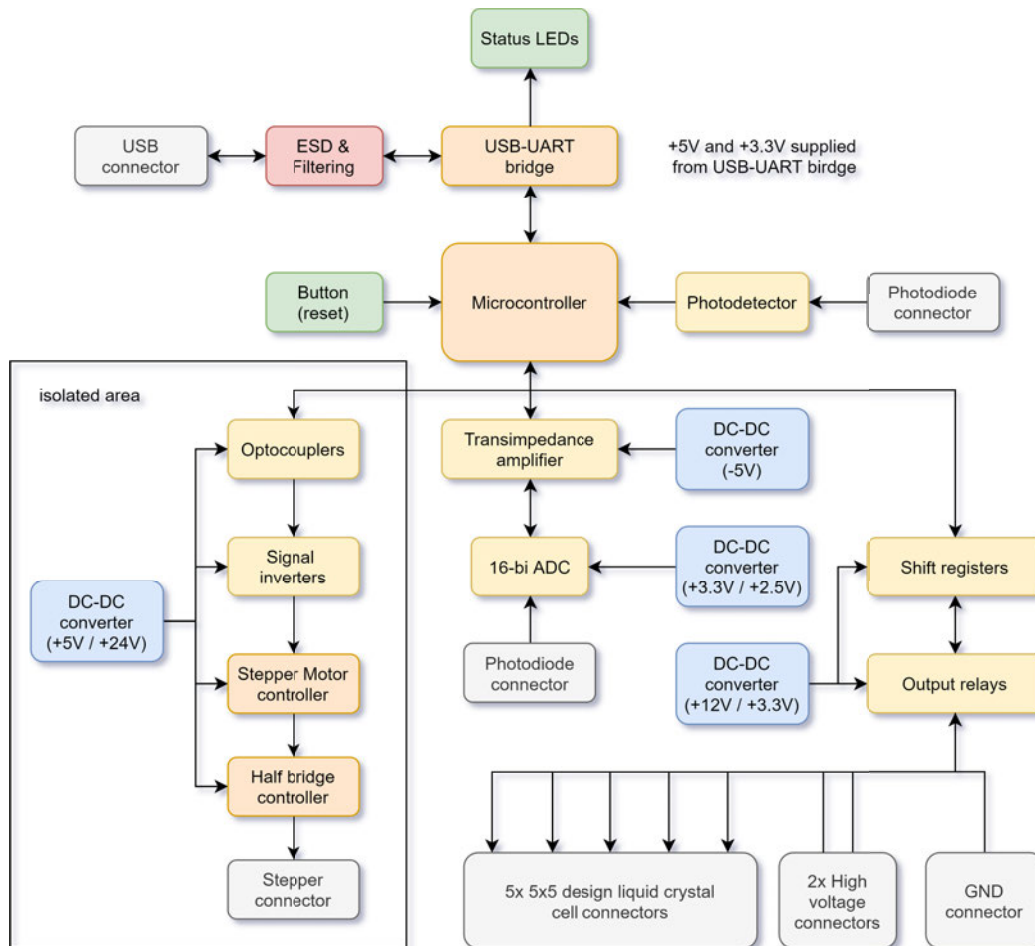
Fig. 7.4. OPMP hardware block diagram.
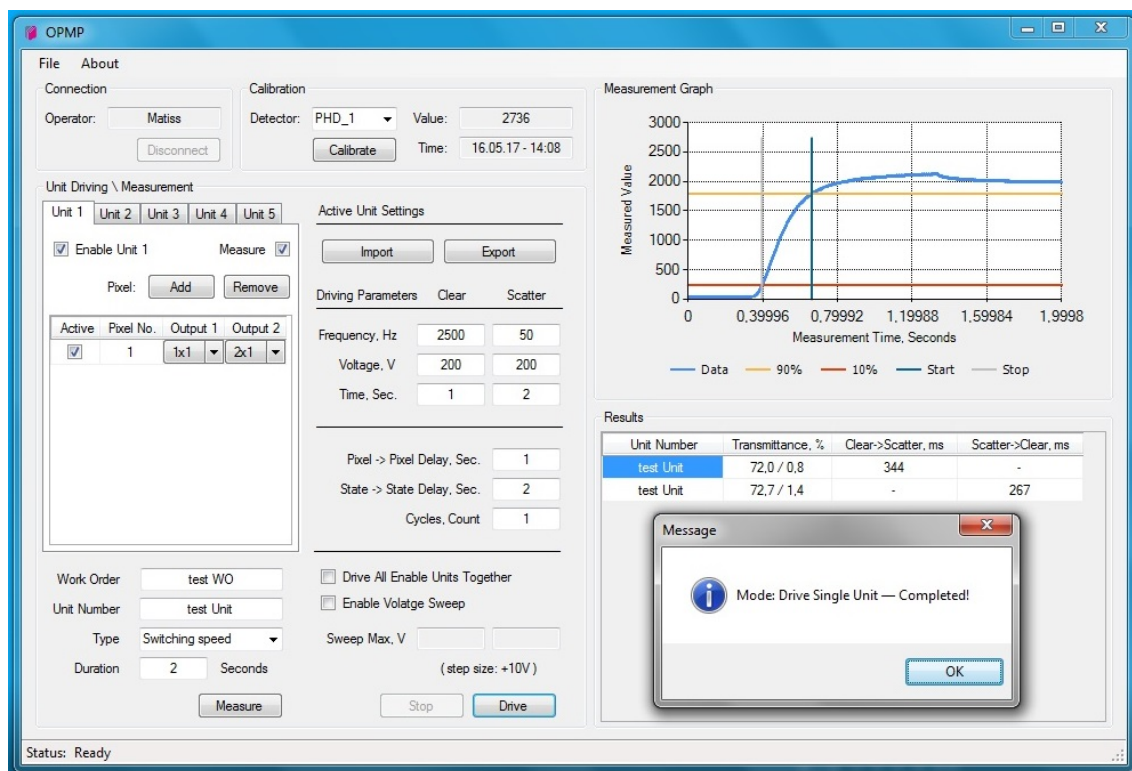
Fig. 7.5. Screenshot of OPMP software.

(a) - front side.

(b) - rear side

Fig. 7.6. OPMP and switching matrix finished enclosure.

7.3.2 Smart glass driver

Smart Glass driver is industrial type *SmA LC* cell driver, designed for large-scale installations, i. e. one device can switch simultaneously two 300×400mm *LC* cells and it is possible to connect 254 devices in series, as well as communicate remotely with each of them individually, see Figure 7.7. For example, if building façade is created with such windows, they can be controlled individually or in groups from a single computer. At the moment custom PC software is only available, but in near future mobile app can be created to improve interaction with the system. Additional sensors can be added to automate the system, i. e., add light sensors to track the movement of the sun and gradually switch *SmA LC* smart windows to the light scattering state.
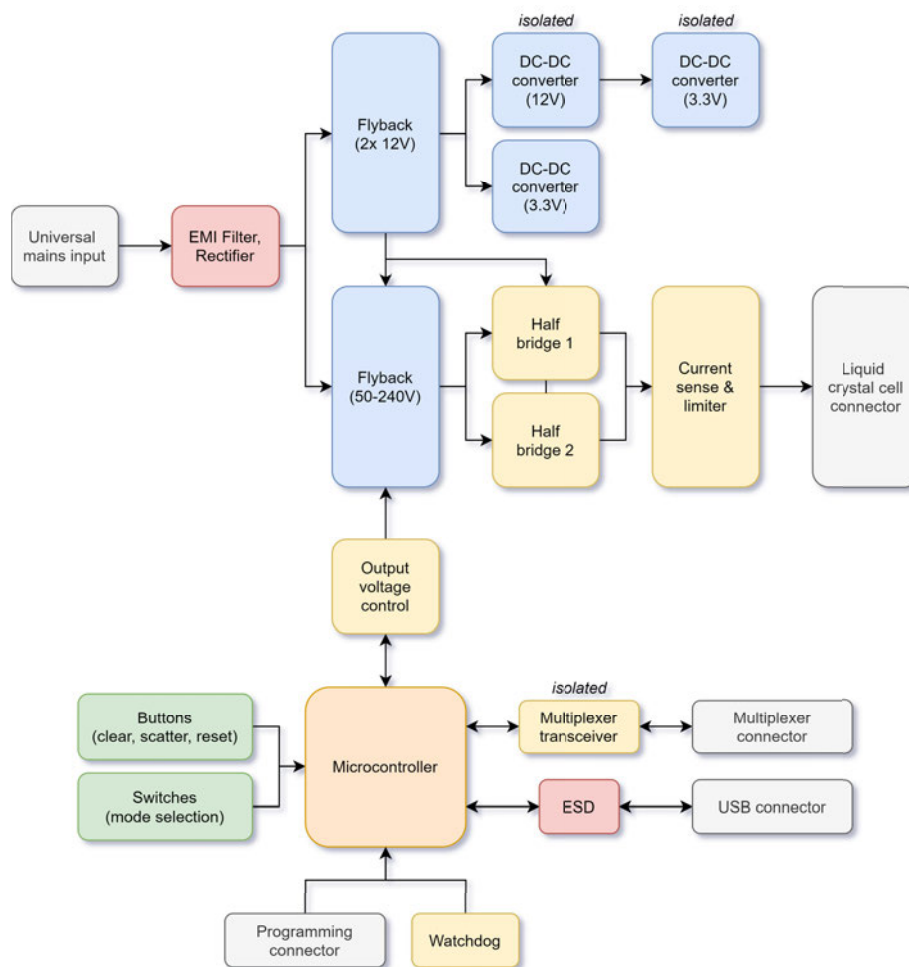
Fig. 7.7. SGD hardware block diagram.

Another example, *SmA LC* smart window used as commercial advert, i. e., some of the *LC* cells can control the incoming light into the commercial premises and others used as signs where image is projected on them or *LC* cell itself is used to show required information or images.

SGD (smart glass driver) can be controlled manually using on-board buttons and five different functions can be pre-programmed, selected via dip switches. The device design

66

is small and compact, so that it can be mounted into ceilings, walls, window frames or left exposed. It is possible to extend manual functionality by adding external buttons/switches and integrate into walls, furniture, etc. for better interaction, see Figure 7.8.

Also, the device is able to change and adjust the waveform of the output signal as needed, e. g., if a new *SmA LC* cell design is developed and requires a modified waveform or switching signal overdrive is needed to improve switching speed, optical properties or is necessary to provide basic functionality, then the existing device will deal with the adjustments needed.
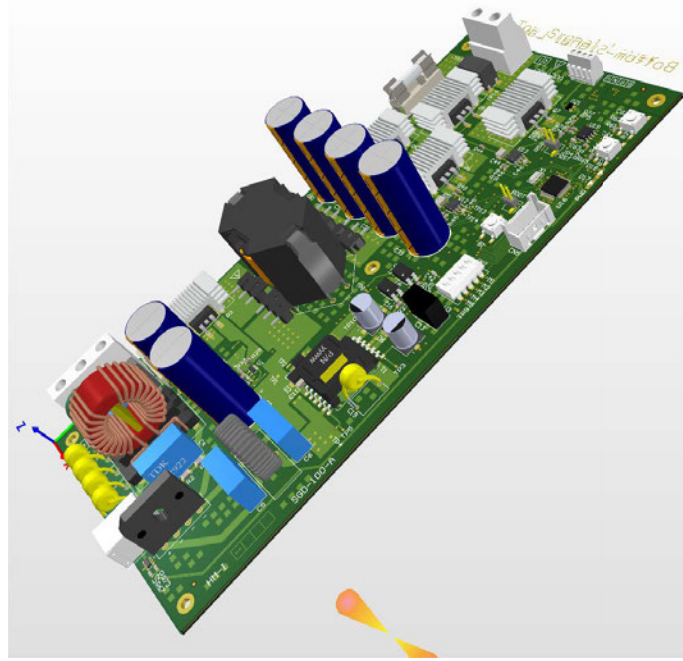
Fig. 7.8. Screenshot of SGD 3D model.

7.4. Upgrade

7.4.1 LC capillary filling

SmA LC cell capillary filling process is very complicated process, because the LC needs to be melted with the right temperature and *LC* cell must be heated in order to allow LC flow. To achieve better heating and temperature control, external heating element mounting was not an option, they needed to be integrated into filling trays. It is necessary to obtain the crystal in a liquid state, heat the LC accordingly to such a temperature that the process is possible, but at the same time it is not damaged or overheated.

The created design allows the use of different types of heating elements, inserted from both ends, as well as various volume filling trays are available. New design (see figure 7.9) allows to perform experiments and filling only a certain number of samples, such as 1x, 4x, 12x, or 16 at the same time. There is also an additional edge, where the crystal can drain and not contaminate the vacuum chamber, facilitating the cleaning processes.
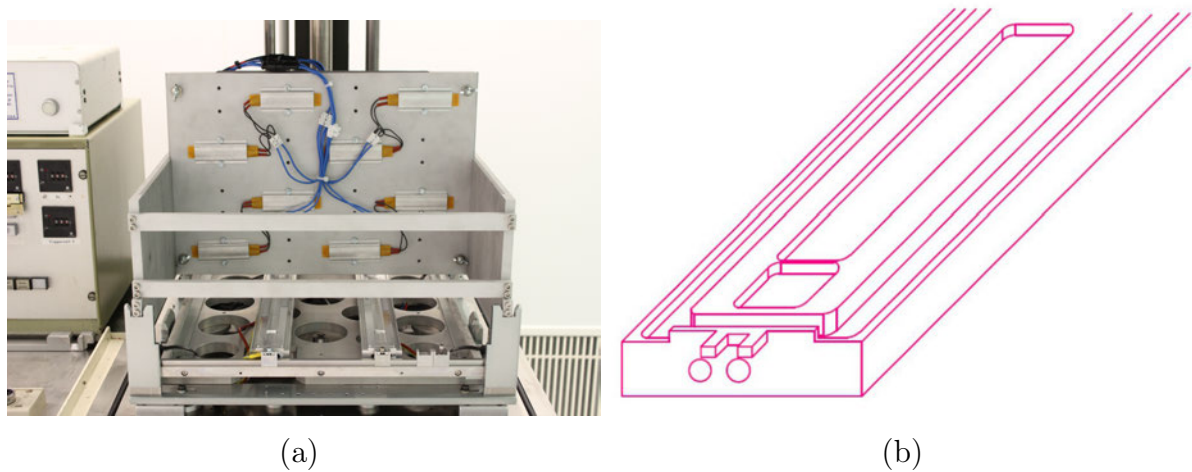
Fig. 7.9. *SmA LC* capillary filling upgrade: (a) - *LC* cell heating plates with external heating elements and LC filling trays in vacuum chamber, (b) - screenshot of 2D drawing of LC filling tray close-up.

7.5. Summary

SmA LC manufactured products, overview of developed hardware and created upgrades for the manufacturing process have been provided within the chapter.

One of the products can bee seen at the Kurzemes Demo Center, others were presented at various events and exhibitions. Each of the products were created for a specific purpose. *SmA LC* cells can be used either as buildings windows, information or speed limit signs, parking lot numbers or simply as a décor element on the wall/table, etc.

The OPMP device allows to perform the functional verification of the manufactured *LC* cells, as well as evaluate and compare *LC* cells side by side. OPMP can functionally verify up to 5 samples at the same time. If it is necessary perform other experiments and can be adapted to different needs.

SGD driver development open up new possibilities to combine *SmA LC* cells and create new products with different complexity and/or integrate them into existing solutions. Device can switch two 300×400mm cells simultaneously with driving waveforms of any shape up to 240 V DC. SGDs' can be connected in series and remotely controlled individually or in pre-defined groups if needed.

The new design of the LC filling trays allow more accurate LC heating and control, as well as make it possible to more efficiently use the available LC volume, i. e., there is no need to fill one or two samples on large tray, on the contrary, a certain size filling tray can be used. New *SmA LC* cell heating plates provide even and accurate heating over the entire surface area.

SmA LC products currently are not available for general use and will not be adapted for mass production, therefore existing knowledge "opens doors" for new experiments and further research.

CONCLUSIONS

The aim of the doctoral thesis was to provide research on the *SmA LC*'s functional behaviour and potential to become the next generation product, that could improve society's daily life. The author has obtained following results:

1. **Explored the light transmittance and switching speed on *SmA LC* cells, depending on the switching frequency.** *SmA LC* cell is frequency depended, which requires specific Hz and signal waveform to reach certain light transmittance values. The frequency range for switching to scattering state is very narrow (10-60 Hz) compared to the frequency range for switching to the transparent state (200-1.5 kHz). The inner state can be achieved within 60-100 Hz frequency range, i. e., *SmA LC* cell will stay in-between light scattering and transparent state. To achieve the highest switching speed (≈1300-1700 ms) and the lowest light transmittance (≈1-1.8 %) in scattering state *SmA LC* should be switched within 20-40 Hz frequency range. And 400-700 Hz frequency range is the most suitable for transparent state, where the light transmittance stays within 85 % and the switching speed varies between 115-150 ms.

2. **Explored power consumption based on switching area.** The power consumption increases exponentially depending on the number of pixels being used. The power consumption reaches the highest point during the transition to a transparent state whilst the whole *SmA LC* cell area is switched. The consumed watt-hour for one switching to the transparent state for a full *LC* cell is ≈0.11 Wh, e. g., *SmA LC* cell consumes approximately the same power amount as two 8.5 W LED bulbs. The *SmA LC* cell (8 pixels, 300 × 400mm) require at least 0.9 A of current to switch whole area from scattering to transparent state and obtain >85 % light transmittance.

3. **Explored switching differences between different *LC* cell design types.** *SmA LC* cells with 8 × 1 designs tend to have more pronounced laser ablation lines, i. e., LC, near these lines, with time will have better optical properties – lower light transmittance compared to the rest of pixels' active area. Pixels edges tend to be more rugged then straight line. 5 × 5 design or similar chess patterned layouts will have problems with switching sequence, image or text displaying. LC tends to create zones, clusters near laser ablation lines. Pixels that are next to the pixel that is being switched, will start to randomly change their state and create random LC clusters. *SmA LC* cells are sensitive to the switching parameters, due to the low parallel resistance, they tend to warm up with intensive switching from state to state. Switching speed rises and *LC* cell stays within the inner state. *SmA LC* cells will never often and quickly change their states without specified pause in-between switching steps - only in cases where testing procedure requires to understand LC degradation boundaries.

4. **Explored LC defect types, their appearance reasons and possible solutions.** In addition to previously mentioned 8×1 and 5×5 design defects, *SmA LC* cells had non uniform active area, some with wavy pattern. Visually sharp light scattering differences, LC did not completely change its state, stuck in the inner state (LC clusters with different light transmittance values near each other). In both states (transparent and scatter) these regions could not be completely switched to either state. With switching parameter and testing cycle optimization it is possible to improve different type defect visual conditions, by adding additional pauses (1-5 s) between pixel-pixel and state-state switching, e. g., pixels wavy outline and rugged edges. These defects tend to return after X number of cycles, but are less pronounced. Unevenly changed area from transparent to scatter state near the laser ablation lines can only be partially improved, non of the experiments, testing methods and optimizations showed any potentials to completely eliminate this problem. With the naked eye it is practically impossible to see this defect in transparent sate, but in scatter state with special attention to the lines defect can be noticed. Similar result was obtained for uneven (discoloured) active area and was partially improved. Defect is related to the production of the display and the methods used there. Manufacturing processes must be optimized to avoid such a defect. Temperature treatment proved that it is possible to "restart" the *SmA LC* cell after being damaged with incorrect switching parameters, testing sequence or other unknown source. This method should be used only if defect could not be fixed with switching optimization. Procedure should be tested and verified with defected *LC* cells to understand if other type of defects could also be fixed.

5. **Explored equivalent load representation options for electronic sub-system simulations.** Obtained results of series R_S and parallel resistance R_P show that R_S stays within provided ITO tolerances (± 20 %) and do not depend on the applied voltage. R_P resistance is lower compared to other *LC* cell parallel resistance, e. g., cholesteric *LC* cell. Great attention should be paid to the power dissipation, with such a low internal parallel resistance LC can quickly reach its temperature limit and *SmA LC* cell will stop working. Capacitance C measurements provide information about *SmA LC* cells' functional range 100-195 V, at which the applied electric field is high enough to be able to rotate LC molecules and change LC state from transparent to scattering and vice versa. Additional in-depth research should be done in 5-95 V range to fully understand LC molecule threshold voltage at which they start to rotate. Simulation model parameters $R_S = 71 \ \Omega$, $R_P = 13 \ \text{k}\Omega$, $C = 53 \ \text{nF}$ will provide sufficient information about electric functionality of large size 300×400 mm *SmA LC* cell and can be integrated into the development of larger systems. This methodology can also be adapted to other *LC* cell types and used to create new electric simulation models.

BIBLIOGRAPHY

[1] W. L. McMillan, "Simple molecular model for the smectic A phase of liquid crystals," *Physical Review A*, vol. 4, no. 3, pp. 1238–1246, 1971.

[2] D. Krishnamurti and H. S. Subramhanyam, "POLARIZATION FIELD AND MOLECULAR ORDER IN SMECTIC LIQUID CRYSTALS." *Mol Cryst Liq Cryst*, vol. 31, no. 1-2, pp. 153–159, 1975.

[3] J. W. Doane, R. S. Parker, B. Cvikl, D. L. Johnson, and D. L. Fishel, "Possible second-order nematic-smectic-A phase transition," *Physical Review Letters*, vol. 28, no. 26, pp. 1694–1696, 1972.

[4] O. Parodi, "A possible magnetic transition in smectics A," *Solid State Communications*, vol. 11, no. 11, pp. 1503–1507, 1972.

[5] K. Miyano and J. B. Ketterson, "Anisotropic ultrasound propagation in a smectic-A liquid crystal," *Physical Review Letters*, vol. 31, no. 17, pp. 1047–1050, 1973.

[6] N. A. Clark and P. S. Pershan, "Light scattering by deformation of the plane texture of smectic and cholesteric liquid crystals," *Physical Review Letters*, vol. 30, no. 1, pp. 3–6, 1973.

[7] A. Takase, S. Sakagami, and M. Nakamizo, "LIGHT SCATTERING STUDY ON ORIENTATIONS IN THE SMECTIC MODIFICATIONS." *Mol Cryst Liq Cryst*, vol. 22, no. 1-2, pp. 67–76, 1973.

[8] P. G. DeGennes, "Viscous flow in smectic A liquid crystals," *Physics of Fluids*, vol. 17, no. 9, pp. 1645–1654, 1974.

[9] M. Hareng, S. Le Berre, and L. Thirant, "Electric field effects on biphenyl smectic A liquid crystals," *Applied Physics Letters*, vol. 25, no. 12, pp. 683–685, 1974.

[10] C. S. Rosenblatt, R. Pindak, N. A. Clark, and R. B. Meyer, "PARABOLIC FOCAL CONIC: A NEW SMECTIC A DEFECT." *J Phys (Paris)*, vol. 38, no. 9, pp. 1105–1115, 1977.

[11] M. Hareng, S. L. Berre, B. Mourey, P. C. Moutou, J. N. Perbet, and L. Thirant, "The Direct-View Matrix-Addressed Smectic A LCD Panel: Dynamic Behavior," *IEEE Transactions on Electron Devices*, vol. 30, no. 5, pp. 507–513, 1983.

[12] M. Hareng, S. Le Berre, R. Hehlen, and J. N. Perbet, "FLAT MATRIX ADDRESSED SMECTIC LIQUID CRYSTAL DISPLAY." in *Digest of Technical Papers - SID International Symposium (Society for Information Display)*, vol. 1. Lewis Winner, 1981, pp. 106–107.

[13] S. Le Berre, M. Hareng, R. Hehlen, and J. N. Perbet, "Flat smectic liquid crystal display panel," *Displays*, vol. 2, no. 7, pp. 349–351, oct 1981.

[14] S. Lu and D. H. Davies, "THERMALLY AND ELECTRICALLY ADDRESSED DYE SWITCHING LCDs." *Molecular crystals and liquid crystals*, vol. 94, no. 1-2, pp. 167–189, 1983.

[15] A. Hochbaum, "Thermally Addressed Smectic Liquid Crystal Displays," *Optical Engineering*, vol. 23, no. 3, jun 1984.

[16] M. Hareng, R. Hehlen, S. Le Berre, J. P. Le Pesant, and L. Thirant, "SMECTIC LIQUID CRYSTAL PANEL FOR TELEVISION PROJECTION." in *Electronic Displays and Information Display Systems.* Network Events Ltd, 1984, pp. 81–91.

[17] Y. Nagae, E. Kaneko, Y. Mori, H. Kawakami, and T. Hashimoto, "FULL-COLOR LASER-ADDRESSED SMECTIC LIQUID-CRYSTAL PROJECTION DISPLAY." *Proceedings of the SID*, vol. 28, no. 1, pp. 55–58, 1986.

[18] K. Liu and K. H. Yang, "ELECTRODE CONFIGURATIONS TO REDUCE THE POWER CONSUMPTION AND ENHANCE THE CONTRAST OF THE MATRIX-ADDRESSED SMECTIC A LIQUID CRYSTAL DISPLAY." *IBM technical disclosure bulletin*, vol. 27, no. 7 B, pp. 4145–4148, dec 1984.

[19] W. A. Crossland and S. Canter, "LARGE FLAT PANEL DISPLAYS USING SMECTIC MEMORY LCDs." *Electronic Engineering (London)*, vol. 57, no. 704, aug 1985.

[20] S. Canter, T. ITT, and W. A. Crossland, "ELECTRICALLY ADDRESSED SMECTIC STORAGE DEVICE FOR LARGE FLAT PANEL DISPLAYS." *Electrical communication*, vol. 60, no. 1, pp. 87–93, 1986.

[21] D. F. Aliev and G. M. Bairamov, "SMECTIC LIQUID CRYSTALS IN COLOR IMAGE DISPLAYS." *Soviet physics. Technical physics*, vol. 28, no. 9, pp. 1086–1087, 1983.

[22] G. Andersson, I. Dahl, P. Keller, W. Kuczyński, S. T. Lagerwall, K. Skarp, and B. Stebler, "Submicrosecond electro-optic switching in the liquid-crystal smectic A phase: The soft-mode ferroelectric effect," *Applied Physics Letters*, vol. 51, no. 9, pp. 640–642, 1987.

[23] T. A. Lobko, B. I. Ostrovskii, A. I. Pavluchenko, and S. N. Sulianov, "X-ray diffraction study of smectic A layering in terminally fluorinated liquid crystal materials," *Liquid Crystals*, vol. 15, no. 3, pp. 361–376, jul 1993.

[24] H. Okada, M. Shibata, and H. Onnagawa, "Investigation of time-resolved x-ray diffraction analysis in smectic a liquid crystal cells," *Japanese Journal of Applied Physics, Part 1: Regular Papers and Short Notes and Review Papers*, vol. 35, no. 10, pp. 5426–5427, 1996.

[25] A. S. Morse and H. F. Gleeson, "Observation of a chevron hybrid structure in the smectic A phase of a liquid crystal device," *Liquid Crystals*, vol. 23, no. 4, pp. 531–535, 1997.

[26] J. Naciri, S. Méry, S. Pfeiffer, and R. Shashidhar, "Novel ferroelectric liquid-crystalline polymers with fast electro-optic switching times," *Journal of the Society for Information Display*, vol. 2, no. 4, p. 175, 1994.

[27] V. Percec and G. Johansson, "Self-regulated phase transitions in poly(4-{2-[4'-(11- vinyloxyundecyloxy)biphenyl-4-yl]ethyl}benzo-15-crown-5) and poly(4-{2-[4'-(11-methacryloylundecyloxy)biphenyl-4-yl]ethyl} benzo-15-crown-5) via molecular recognition," *Journal of Materials Chemistry*, vol. 3, no. 1, pp. 83–96, 1993.

[28] J. Wen, M. Tian, Z. Guo, and Q. Chen, "Synthesis and phase-transition of 4-alkoxycarbonylphenyl 4'-n-alkoxy-2, 3, 5, 6-tetrafluorobiphenyl-4-carboxylates," *Molecular Crystals and Liquid Crystals Science and Technology Section A: Molecular Crystals and Liquid Crystals*, vol. 275, pp. 27–36, 1996.

[29] M. Bardosova, S. D. Evans, P. Hodge, V. Jablonska, S. Johnson, and R. H. Tredgold, "Ultra-thin films of polymerised smectic liquid crystals. A study using AFM and ellipsometry," *Materials Science and Engineering C*, vol. 8-9, pp. 85–87, dec 1999.

[30] H. Yang, H. Yamane, H. Kikuchi, H. Yamane, G. Zhang, X. Chen, and K. Tisato, "Investigation of the electrothermo-optical effect of a smectic LCP-nematic LC-chiral dopant ternary composite system based on SA ↔ N* phase transition," *Journal of Applied Polymer Science*, vol. 73, no. 5, pp. 623–631, 1999.

[31] J. W. Naciri, B. T. Weslowski, C. Wilson, R. Shashidhar, and B. R. Ratna, "Advances in liquid crystals for gray-scale applications," in *Liquid Crystal Materials, Devices, and Applications VII*, Jawad W. Naciri, Brian T. Weslowski, C. Wilson, Ranganathan Shashidhar, and Banahalli R. Ratna, Eds., vol. 3635. SPIE, mar 1999, pp. 8–13. [Online]. Available: http: //proceedings.spiedigitallibrary.org/proceeding.aspx?articleid=978559

[32] V. L. Aristov, M. V. Mitrokhin, and V. P. Sevostyanov, "Analysis of destructive physicochemical processes in optical media of liquid crystal displays," in *1998 4th International Conference on Actual Problems of Electronic Instrument Engineering,*

APEIE 1998 - Proceedings, vol. 1998-Septe. Institute of Electrical and Electronics Engineers Inc., 1998, pp. 199–200.

[33] V. L. Aristov, S. P. Kurchatkin, M. V. Mitrokhin, and V. P. Sevostyanov, "Fringe optical distortion of LCD pixels," in *Liquid Crystals: Physics, Technology, and Applications*, vol. 3318. SPIE, feb 1998, p. 523.

[34] P. Rudquist, M. Buivydas, L. Komitov, and S. T. Lagerwall, "Linear electro-optic effect based on flexoelectricity in a cholesteric with sign change of dielectric anisotropy," *Journal of Applied Physics*, vol. 76, no. 12, pp. 7778–7783, 1994.

[35] D. F. Aliev, V. L. Aristov, V. V. Mitrokhin, and V. P. Sevostyanov, "Operating characterization of a smectic A LCD," *Displays*, vol. 12, no. 2, pp. 86–90, 1991.

[36] S. S. Seomun, Y. Takanishi, K. Ishikawa, H. Takezoe, and A. Fukuda, "Evolution of switching characteristics from tristable to V-shaped in an apparently antiferroelectric liquid crystal," *Japanese Journal of Applied Physics, Part 1: Regular Papers and Short Notes and Review Papers*, vol. 36, no. 6 A, pp. 3586–3590, 1997.

[37] V. L. Aristov, S. P. Kurchatkin, M. V. Mitrokhin, and V. P. Sevostyanov, "Electrohydrodynamic formation of liquid crystal focal conic domains," in *Liquid Crystals: Physics, Technology, and Applications*, vol. 3318. SPIE, feb 1998, p. 529.

[38] T. Inoue and S. Mikoshiba, "High density data recording on thermally addressable liquid crystal for three-dimensional holographic display," *Japanese Journal of Applied Physics, Part 1: Regular Papers and Short Notes and Review Papers*, vol. 38, no. 12 A, pp. 6757–6761, dec 1999.

[39] V. L. Aristov, M. V. Mitrokhin, V. P. Sevost'yanov, and M. G. Tomilin, "Liquid-crystal displays based on the electrically controllable light-scattering effect in smectic A liquid crystals," *Journal of Optical Technology (A Translation of Opticheskii Zhurnal)*, vol. 65, no. 7, pp. 573–576, 1998.

[40] W. Saito and A. Baba, "Rewritable medium using smectic A polymer dispersed liquid crystal films," *Kyokai Joho Imeji Zasshi/Journal of the Institute of Image Information and Television Engineers*, vol. 53, no. 8, pp. 1142–1146, 1999.

[41] V. L. Aristov, S. P. Kurchatkin, M. V. Mitrokhin, and V. P. Sevostyanov, "Field-controlled light scattering from polymer-dispersed liquid crystal displays," in *Liquid Crystals: Physics, Technology, and Applications*, vol. 3318. SPIE, feb 1998, p. 526.

[42] A. Findon, H. Gleeson, and J. Lydon, "Realignment of a smectic-A phase with applied electric field," *Physical Review E - Statistical Physics, Plasmas, Fluids, and Related Interdisciplinary Topics*, vol. 62, no. 4, pp. 5137–5142, 2000.

[43] T. K. Misra and L. J. Martínez-Miranda, "Effects of electric fields as a function of depth in a smectic film," in *Molecular Crystals and Liquid Crystals*, vol. 412, 2004.

[44] L. J. Martínez-Miranda and Y. Hu, "Temperature and depth dependence of order in liquid crystal interfaces," *Journal of Applied Physics*, vol. 99, no. 11, jun 2006.

[45] D. Liang and R. L. Leheny, "Smectic liquid crystals in an anisotropic random environment," *Physical Review E - Statistical, Nonlinear, and Soft Matter Physics*, vol. 75, no. 3, mar 2007.

[46] D. J. Gardiner and H. J. Coles, "Optimization of organosiloxane mesogenic properties for use in a smectic-A display," in *Emerging Liquid Crystal Technologies*, vol. 5741. SPIE, apr 2005, p. 239.

[47] ——, "Organosiloxane liquid crystals for fast-switching bistable scattering devices," *Journal of Physics D: Applied Physics*, vol. 39, no. 23, pp. 4948–4955, dec 2006.

[48] N. Gheorghiu, J. L. West, A. V. Glushchenko, and M. Mitrokhin, "Patterned field induced polymer walls for smectic A bistable flexible displays," *Applied Physics Letters*, vol. 88, no. 26, 2006.

[49] E. A. Büyüktanir, N. Gheorghiu, J. L. West, M. Mitrokhin, B. Holter, and A. Glushchenko, "Field-induced polymer wall formation in a bistable smectic-A liquid crystal display," *Applied Physics Letters*, vol. 89, no. 3, 2006.

[50] V. L. Aristov, M. V. Mitrokhin, and M. G. Tomilin, "How the structure of a smectic-A liquid crystal affects the spectral characteristics of transmitted light," *Journal of Optical Technology*, vol. 70, no. 7, p. 474, jul 2003.

[51] M. V. Mitrokhin, L. Johnsen, R. Fagerberg, C. Kristiansen, F. J. Farrand, K. H. Holm, R. Palm, K. Netland, and V. L. Aristov, "Prevention of smectic-A LC mixtures electrolytic degradation," in *Molecular Crystals and Liquid Crystals*, vol. 411, 2004.

[52] H.-Y. Chen, R. Shao, E. Korblova, D. Walba, N. A. Clark, and W. Lee, "Bistable SmA liquid-crystal display driven by a two-direction electric field," *Journal of the Society for Information Display*, vol. 16, no. 6, p. 675, 2008.

[53] V. L. Aristov, M. V. Mitrokhin, V. P. Sevostyanov, and M. G. Tomilin, "Features of the control of array-type liquid-crystal memory displays," *Journal of Optical Technology*, vol. 68, no. 9, p. 660, sep 2001.

[54] D. J. Gardiner and H. J. Coles, "Enhancing lifetime in a bistable smectic A liquid crystal device," *Journal of Physics D: Applied Physics*, vol. 40, no. 4, pp. 977–981, feb 2007.

[55] H. Y. Chen, R. Shao, E. Korblova, W. Lee, D. Walba, and N. A. Clark, "A bistable liquid-crystal display mode based on electrically driven smectic A layer reorientation," *Applied Physics Letters*, vol. 91, no. 16, 2007.

[56] D. J. Gardiner, C. J. Davenport, J. Newton, and H. J. Coles, "Electro-optic bistability in organosiloxane bimesogenic liquid crystals," *Journal of Applied Physics*, vol. 99, no. 11, jun 2006.

[57] V. L. Aristov, M. V. Mitrokhin, and V. P. Sevostyanov, "Temperature influence on electrooptical and switching properties of polymer dispersed smectic a liquid crystal displays," in *SID Conference Record of the International Display Research Conference*, 2000, pp. 205–208.

[58] B. Holter, T. G. Kamfjord, R. Fossum, and R. Fagerberg, "Flexible daylight memory displays EASL DMD: a new approach toward displays for cockpit and soldier systems," in *Cockpit Displays VII: Displays for Defense Applications*, vol. 4022. SPIE, aug 2000, pp. 227–232.

[59] E. A. Büyüktanir, A. Glushchenko, B. Wall, J. L. West, M. Mitrokhin, and B. Holter, "Flexible Bistable Smectic-A LCD Based on PDLC," *SID Symposium Digest of Technical Papers*, vol. 36, no. 1, p. 1778, 2005.

[60] M. V. Mitrokhin and B. Holter, "Reflective Bistable Smectic-A Passive Matrix LCDs," *SID Symposium Digest of Technical Papers*, vol. 36, no. 1, p. 1774, 2005.

[61] E. A. Büyüktanir, M. Mitrokhin, B. Holter, A. Glushchenko, and J. L. West, "Flexible bistable smectic-A polymer dispersed liquid crystal display," *Japanese Journal of Applied Physics, Part 1: Regular Papers and Short Notes and Review Papers*, vol. 45, no. 5 A, pp. 4146–4151, may 2006.

[62] M. V. Mitrokhin, S. Bragstad, B. Holter, and B. G. Wall, "Bistable Smectic-A LCDs: Paper-Like Reflective and See-Through Transmissive Modes," *SID Symposium Digest of Technical Papers*, vol. 37, no. 1, p. 283, 2006.

[63] D. J. Gardiner, S. M. Morris, and H. J. Coles, "High-efficiency multistable switchable glazing using smectic A liquid crystals," *Solar Energy Materials and Solar Cells*, vol. 93, no. 3, pp. 301–306, mar 2009.

[64] M. V. Mitrokhin, L. Johnsen, R. Fagerberg, B. Holter, and V. L. Arisov, "Adsorption processes during the filling of a display with a smectic A LC mixture," *Liquid Crystals*, vol. 31, no. 3, pp. 317–324, mar 2004.

[65] C. Jones, "Bistable liquid crystal displays," in *Handbook of Visual Display Technology*. Springer Berlin Heidelberg, jan 2012, vol. 3, pp. 1507–1538.

[66] H. P. Hinov, *Electro-optic effects in thermotropic liquid crystals*. Nova Science Publishers, Inc., apr 2015.

[67] H. Xu, A. B. Davey, W. A. Crossland, and D. P. Chu, "UV durable colour pigment doped SmA liquid crystal composites for outdoor trans-reflective bi-stable displays," in *Liquid Crystals XVI*, vol. 8475. SPIE, oct 2012, p. 847506.

[68] W. Ji, L.-Y. Shi, H. Tang, G. Sun, W. Hu, and X. Liang, "Large birefringence smectic-A liquid crystals for high contrast bistable displays," *Optical Materials Express*, vol. 5, no. 2, p. 281, feb 2015.

[69] J. W. Huh, T. H. Choi, J. H. Kim, J. H. Woo, J. H. Seo, and T. H. Yoon, "Bistable Switching of Diffractive Smectic-A Liquid Crystal Device between Haze-Free Transparent and High-Haze Translucent States," *ACS Photonics*, vol. 5, no. 8, pp. 3152–3158, aug 2018.

[70] R. Dabrowski, J. Dziaduszek, J. Bozetka, W. Piecek, R. Mazur, M. Chrunik, P. Perkowski, M. Mrukiewicz, M. Żurowska, and D. Weglowska, "Fluorinated smectics – New liquid crystalline medium for smart windows and memory displays," *Journal of Molecular Liquids*, vol. 267, pp. 415–427, oct 2018.

[71] G. Mozolevskis, E. Nitiss, and A. Medvids, "Electric breakdown of dielectric thin films for high-voltage display applications," in *Holography, Diffractive Optics, and Applications VII*, vol. 10022. SPIE, oct 2016, p. 100222S.

[72] Y. Lu, J. Guo, H. Wang, and J. Wei, "Flexible bistable smectic-A liquid crystal device using photolithography and photoinduced phase separation," *Advances in Condensed Matter Physics*, vol. 2012, 2012.

[73] H.-Y. Chen and J.-S. Wu, "A multistable smectic-A liquid-crystal device with low threshold field," *Journal of the Society for Information Display*, vol. 18, no. 6, p. 415, 2010.

[74] K. Peddireddy, V. S. R. Jampani, S. Herminghaus, C. Bahr, M. Vitek, and I. Muševič, "Lasing and waveguiding in smectic A liquid crystal optical fibers," in *Liquid Crystals XVIII*, vol. 9182. SPIE, oct 2014, p. 91820Y.

[75] A. Honglawan, D. A. Beller, M. Cavallaro, R. D. Kamien, K. J. Stebe, and S. Yang, "Topographically induced hierarchical assembly and geometrical transformation of focal conic domain arrays in smectic liquid crystals," *Proceedings of the National Academy of Sciences of the United States of America*, vol. 110, no. 1, pp. 34–39, jan 2013.

[76] D. A. Beller, M. A. Gharbi, A. Honglawan, K. J. Stebe, S. Yang, and R. D. Kamien, "Focal conic flower textures at curved interfaces," *Physical Review X*, vol. 3, no. 4, 2014.

[77] F. Reinitzer, "Beiträge zur Kenntniss des Cholesterins," *Monatshefte für Chemie*, vol. 9, no. 1, pp. 421–441, dec 1888. [Online]. Available: https://link.springer.com/article/10.1007/BF01516710

[78] T. J. Sluckin, D. A. Dunmur, and H. Stegemeyer, *Crystals That Flow: Classic Papers from the History of Liquid Crystals*. CRC Press, jun 2004.

[79] Y. Tabe, K. Urayama, A. Matsuyama, J. Yamamoto, and M. Yoneya, "Physics of liquid crystals," in *The Liquid Crystal Display Story: 50 Years of Liquid Crystal R and D that Lead the Way to the Future*. Springer Japan, jan 2014, pp. 301–356. [Online]. Available: https://link.springer.com/chapter/10.1007/978-4-431-54859-1{_}10

[80] P. G. de Gennes and J. Prost, *The Physics of Liquid Crystals*, 2nd ed. Clarendon Press, 1995. [Online]. Available: https://global.oup.com/academic/product/the-physics-of-liquid-crystals-9780198517856?cc=lv{\\&}lang=en{\\&}{\\#}

[81] D. Dunmur, A. Fukuda, and G. Luckhurst, *Physical Properties of Liquid Crystals*. Institution of Engineering and Technology, 2001. [Online]. Available: https://www.waterstones.com/book/physical-properties-of-liquid-crystals/d-a-dunmur/a-fukuda/9780852967843

[82] I.-C. Khoo and S.-T. Wu, *Optics and Nonlinear Optics of Liquid Crystals*. WORLD SCIENTIFIC, apr 1993.

[83] L. M. Blinov and V. G. Chigrinov, *Electrooptic Effects in Liquid Crystal Materials*, ser. Partially Ordered Systems. New York, NY: Springer New York, 1994. [Online]. Available: http://link.springer.com/10.1007/978-1-4612-2692-5

[84] UKEssays, "Classifications of Liquid Crystals," 2018. [Online]. Available: https://www.ukessays.com/essays/chemistry/classifications-liquid-crystals-7625.php

[85] S. Chandrasekhar, *Liquid Crystals*. Cambridge University Press, nov 1992. [Online]. Available: https://www.cambridge.org/core/product/identifier/9780511622496/type/book

[86] E. B. Priestley, P. J. Wojtowicz, and P. Sheng, *Introduction to Liquid Crystals*, 1st ed. Springer US, 1976.

[87] P. J. Collings and A. Hilger, *Liquid crystals: Nature's delicate phase of matter*. Princeton University Press, 1990.

[88] M. P. Petrov, *Optical and Electro-Optical Properties of Liquid Crystals: Nematic and Smectic Phases*. Nova Science Publisher, 2011. [Online]. Available: https://novapublishers.com/shop/optical-and-electro-optical-properties-of-liquid-crystals-nematic-and-smectic-phases/

[89] Gauzy, "Smart Glass - Everything You Want To Know...And More." [Online]. Available: https://www.gauzy.com/smart-glass-everything-you-want-to-know/

[90] D. S. Parmar and J. J. Singh, "Partially exposed polymer dispersed liquid crystals for boundary layer investigations," *Applied Physics Letters*, vol. 61, no. 17, pp. 2039–2041, oct 1992. [Online]. Available: http://aip.scitation.org/doi/10.1063/1.108352

[91] D. S. Parmar and H. K. Holmes, "Skin friction measurement with partially exposed polymer dispersed liquid crystals," *Review of Scientific Instruments*, vol. 64, no. 2, pp. 538–541, feb 1993. [Online]. Available: http://aip.scitation.org/doi/10.1063/1.1144229

[92] C. Shen and T. Kyu, "Spinodals in a polymer dispersed liquid crystal," *The Journal of Chemical Physics*, vol. 102, no. 1, pp. 556–562, jan 1995. [Online]. Available: http://aip.scitation.org/doi/10.1063/1.469435

[93] S. Singh, J. K. Srivastava, and R. K. Singh, "Polymer Dispersed Liquid Crystals," in *Liquid Crystalline Polymers: Volume 1-Structure and Chemistry*. Springer International Publishing, jan 2015, pp. 195–250.

[94] P. S. Drzaic, *Liquid Crystal Dispersions*. WORLD SCIENTIFIC, sep 1995, vol. 1.

[95] A. Puzari, "Liquid crystalline polymer composites for optoelectronics," in *Liquid Crystalline Polymers: Volume 2-Processing and Applications*. Springer International Publishing, jan 2015, pp. 315–338.

[96] R. R. Deshmukh, "Electro-optic and dielectric responses in PDLC composite systems," in *Liquid Crystalline Polymers: Volume 2-Processing and Applications*. Springer International Publishing, jan 2015, pp. 169–195.

[97] E. J. Shin, S. C. Noh, T. H. Kim, J. H. Kim, P. Nayek, M. H. Lee, M. S. Kini, L. C. Chien, J. H. Lee, B. K. Kim, and S. H. Lee, "Enhancement of electro-optic properties of optically isotropic liquid crystal device for flexible display," in *Digest of Technical Papers - SID International Symposium*, vol. 46, no. Book 3. Blackwell Publishing Ltd, jun 2015, pp. 1483–1486.

[98] G. N. Hassanein, N. Kattan, and M. A. Ellabban, "Electro-optic properties of aligned and non-aligned polymer dispersed liquid crystals driven by an amplitude-modulated electric signal," *Optik*, vol. 186, pp. 137–146, jun 2019.

[99] D. Manaila-Maximean, P. Ganea, V. Loiko, A. Konkolovich, V. Cîrcu, O. Dănilă, and A. Bărar, "Polymer dispersed liquid crystals doped with nanoparticles: electric and electro-optical properties," in *Proceedings Volume 11718, Advanced Topics in*

Optoelectronics, Microelectronics and Nanotechnologies X;. SPIE-Intl Soc Optical Eng, dec 2020, p. 121.

[100] G. Y. Shim, H. G. Kim, J. S. Park, D. J. Lee, J. H. Baek, J. H. Lee, B. K. Kim, and H. R. Kim, "Reduction of optical scattering and driving voltage of polymer-dispersed liquid crystals," in *Proceedings of the International Display Workshops*, vol. 1. International Display Workshops, 2015, pp. 406–408.

[101] V. Nimmy John, S. N. Varanakkottu, and S. Varghese, "Flexible, ferroelectric nanoparticle doped polymer dispersed liquid crystal devices for lower switching voltage and nanoenergy generation," *Optical Materials*, vol. 80, pp. 233–240, jun 2018.

[102] C. C. Huang, H. H. Huang, B. W. Liang, C. C. Lee, B. H. Kung, and C. H. Kuan, "Well Arranged PDLC Droplets in Grating Structures Inducing the Reduction of Driving Voltage," in *2019 Conference on Lasers and Electro-Optics, CLEO 2019 - Proceedings.* Institute of Electrical and Electronics Engineers Inc., may 2019.

[103] T.-H. Yoon, J.-W. Huh, J.-H. Kim, Y.-S. Jo, S.-M. Ji, and T.-H. Choi, "Control of the haze value by the electro-hydrodynamic effect in a liquid crystal cell," in *Proceedings Volume 10735, Liquid Crystals XXII;.* SPIE-Intl Soc Optical Eng, sep 2018, p. 25.

[104] H. Manabe, M. Date, H. Takada, and H. Inamura, "Low power driving techniques for 1-pixel displays," in *IEEE Industry Application Society - 51st Annual Meeting, IAS 2015, Conference Record.* Institute of Electrical and Electronics Engineers Inc., dec 2015.

[105] Q. Wu and Y. Wang, "Low driving voltage ITO doped polymer-dispersed liquid crystal film and reverse voltage pulse driving method," *Applied Optics*, vol. 56, no. 29, p. 8159, oct 2017.

[106] C. M. Lampert, "The world of large-area glazing and displays," in *Switchable Materials and Flat Panel Displays*, C. M. Lampert, Ed., vol. 3788, no. 8. SPIE, oct 1999, pp. 2–11. [Online]. Available: http://proceedings.spiedigitallibrary.org/proceeding.aspx?articleid=998292

[107] M. Oltean, "Switchable glass: A possible medium for Evolvable Hardware," in *Proceedings - First NASA/ESA Conference on Adaptive Hardware and Systems, AHS 2006*, vol. 2006. IEEE Computer Society, 2006, pp. 81–87.

[108] R. Vergaz, J. M. Pena, D. Barrios, I. Pérez, and J. C. Torres, "Electrooptical behaviour and control of a suspended particle device," *Opto-electronics Review*, vol. 15, no. 3, pp. 154–158, sep 2007. [Online]. Available: https://www.degruyter.com/document/doi/10.2478/s11772-007-0013-9/html

[109] A. Ghosh, B. Norton, and A. Duffy, "Behaviour of a SPD switchable glazing in an outdoor test cell with heat removal under varying weather conditions," *Applied Energy*, vol. 180, pp. 695–706, oct 2016.

[110] K. W. Goossen and D. Wolfe, "Optofluidic smart glass with wide angular performance," in *The International Society for Optical Engineering*. SPIE, mar 2018, p. 1.

[111] E. Lim, J.-H. Kim, T.-H. Yoon, S.-M. Ji, Y.-S. Jo, S.-M. Nam, J.-W. Huh, S.-W. Oh, and S.-H. Kim, "Transmittance control of a liquid crystal device using a dye mixture," in *Proceedings Volume 10735, Liquid Crystals XXII;*. SPIE, sep 2018, p. 43.

[112] J. Han, M. C. Freyman, E. Feigenbaum, and T. Yong-Jin Han, "Electro-Optical Device with Tunable Transparency Using Colloidal Core/Shell Nanoparticles," *ACS Photonics*, vol. 5, no. 4, pp. 1343–1350, apr 2018.

[113] M. Casini, "Smart windows for energy efficiency of buildings," in *Second International Conference on Advances In Civil, Structural and Environmental Engineering- ACSEE 2014*. Seek, oct 2014, pp. 273–281.

[114] M. Zayat, D. Almendro, V. Vadillo, and D. Levy, "Sol-Gel Optical and Electro-Optical Materials," in *The Sol-Gel Handbook*. Wiley Blackwell, sep 2015, vol. 3-3, pp. 1239–1280.

[115] U. Posset and M. Harsch, "Life Cycle Analysis (LCA) of Electrochromic Smart Windows," in *Electrochromic Materials and Devices*. Wiley Blackwell, jul 2015, pp. 545–570.

[116] K. Yoshimura, "Metal Hydrides for Smart-Window Applications," in *Electrochromic Materials and Devices*. Wiley Blackwell, jul 2015, pp. 241–248.

[117] M. Oh, M. Jang, J. Moon, and S. Roh, "Evaluation of Building Energy and Daylight Performance of Electrochromic Glazing for Optimal Control in Three Different Climate Zones," *Sustainability*, vol. 11, no. 1, p. 287, jan 2019. [Online]. Available: https://www.mdpi.com/2071-1050/11/1/287

[118] B. P. Jelle, "Electrochromic Smart Windows for Dynamic Daylightand Solar Energy Control in Buildings," in *Electrochromic Materials and Devices*. Wiley Blackwell, jul 2015, pp. 419–502.

[119] S. C. Nunes, S. M. Saraiva, R. F. Pereira, S. Pereira, M. M. Silva, L. D. Carlos, E. Fortunato, R. A. Ferreira, R. Rego, and V. De Zea Bermudez, "Sustainable Dual-Mode Smart Windows for Energy-Efficient Buildings," *ACS Applied Energy Materials*, vol. 2, no. 3, pp. 1951–1960, mar 2019.

[120] L. Zheng and K. W. Shah, "Chapter 16: Electrochromic Smart Windows for Green Building Applications," in *RSC Smart Materials*. Royal Society of Chemistry, 2019, vol. 2019-Janua, no. 33, pp. 494–520.

[121] M. Fernandes, V. Freitas, S. Pereira, R. Leones, M. M. Silva, L. D. Carlos, E. Fortunato, R. A. Ferreira, R. Rego, and V. de Zea Bermudez, "Luminescent electrochromic devices for smart windows of energy-efficient buildings," *Energies*, vol. 11, no. 12, dec 2018.

[122] A. Cannavale, U. Ayr, F. Fiorito, and F. Martellotta, "Smart electrochromic windows to enhance building energy efficiency and visual comfort," *Energies*, vol. 13, no. 6, 2020.

[123] W. Haase, M. Husser, and W. Sobek, "Adaptive glazing systems - Survey of systems," in *IEEE/ASME International Conference on Advanced Intelligent Mechatronics, AIM*. Institute of Electrical and Electronics Engineers Inc., aug 2017, pp. 929–933.

[124] D. Papathanasopoulos, G. Leftheriotis, and E. Mitronikas, "Design, fabrication, and testing of an electronic device for the automatic control of electrochromic windows," *Journal of Building Engineering*, vol. 12, pp. 248–258, jul 2017.

[125] Z. ShiQing, H. WenBin, and L. YanHua, "High performance electrochromic device based on multifunctional hydrogel," in *Proceedings Volume 11335, AOPC 2019: Display Technology and Optical Storage;*. SPIE-Intl Soc Optical Eng, dec 2019, p. 11.

[126] V. A. Barachevsky, "2D materials for smart energochromic sunscreen devices," in *2D Nanomaterials for Energy Applications: Graphene and Beyond*. Elsevier, jan 2019, pp. 173–208.

[127] M. Feng, X. Bu, J. Yang, D. Li, Z. Zhang, Y. Dai, and X. Zhang, "Review: smart windows based on photonic crystals," *Journal of Materials Science*, vol. 55, no. 20, pp. 8444–8463, jul 2020.

[128] S. Xi, Y. Chen, Z. Bi, S. Jia, X. Guo, X. Gao, and X. Li, "Energy storage smart window with transparent-to-dark electrochromic behavior and improved pseudocapacitive performance," *Chemical Engineering Journal*, vol. 370, pp. 1459–1466, aug 2019.

[129] J. Bin Lias, T. Naing Oo, T. Yazawa, M. Kimura, and T. Akahane, "Liquid crystal alignment on patterned-alignment films," *Journal of Information Display*, vol. 12, no. 2, pp. 101–107, 2011. [Online]. Available: https://doi.org/10.1080/15980316.2011.567826

[130] J. W. Huh, T. H. Choi, J. H. Kim, J. H. Woo, J. H. Seo, and T. H. Yoon, "Bistable Switching of Diffractive Smectic-A Liquid Crystal Device between Haze-Free Transparent and High-Haze Translucent States," *ACS Photonics*, vol. 5, no. 8, pp. 3152–3158, aug 2018.

[131] G. Mozoļevskis, "DIELECTRIC BREAKDOWN OF HIGH VOLTAGE LIQUID CRYSTAL DISPLAYS," Ph.D. dissertation, RIGA TECHNICAL UNIVERSITY, Riga, 2017.

[132] D. J. Cristaldi, S. Pennisi, and F. Pulvirenti, *Liquid Crystal Display Drivers: Techniques and Circuits*, 1st ed. Springer Science+Business Media B.V., 2009. [Online]. Available: http://www.springer.com/gp/book/9789048122547

[133] E. Lueder, *Liquid Crystal Displays: Addressing Schemes and Electro-Optical Effects*, 2nd ed. Wiley, A John Wiley and Sons, Ltd, Publication, 2010. [Online]. Available: https://www.wiley.com/en-lv/Liquid+Crystal+Displays{\%}3A+Addressing+ Schemes+and+Electro+Optical+Effects{\%}2C+2nd+Edition-p-9780470688182

[134] T. V. Clapp, W. A. Crossland, A. B. Davey, M. Grassman, J. P. Hannington, R. K. King, M. Pivnonenko, S. Robson, and H. Xu, "Liquid crystal formulations and structures for smectic a optical devices," p. 85, 2011. [Online]. Available: http://www.dowcorning.com/content/paintink/paintinkresin/default.aspx

[135] J. P. Hannington, T. V. Clapp, F. Nishida, R. K. King, O. Farooq, M. Grassman, W. A. Crossland, H. J. Coles, A. B. Davey, H. Xu, O. Hadeler, and M. Pivnenko, "Oligosiloxane modified liquid crystal formulations and devices using same (US Patent)," p. 28, 2013.

[136] G. Mozolevskis, A. Ozols, E. Nitiss, E. Linina, A. Tokmakov, and M. Rutkis, "Reduction of Electric Breakdown Voltage in LC Switching Shutters," *Latvian Journal of Physics and Technical Sciences*, vol. 52, no. 5, pp. 47–57, 2015.

[137] K. R. Fowler, *Test and Integration*. Elsevier Inc., 2015. [Online]. Available: http://dx.doi.org/10.1016/B978-0-12-405879-8.00014-3

[138] H. Grzeskowiak, T. Lhommeau, and D. Delaux, "Highly Accelerated Testing," *Reliability of High-Power Mechatronic Systems 2: Aerospace and Automotive Applications Issues, Testing and Analysis*, pp. 57–108, 2017.

[139] E. Suhir, J. Nicolics, and S. Yi, "Failure-oriented-accelerated-testing and its role in making a device into a product," *2019 IEEE International Workshop on Metrology for AeroSpace, MetroAeroSpace 2019 - Proceedings*, pp. 33–38, 2019.

[140] M. Maltisovs, K. Krumins, A. Ozols, and D. Pikulins, "Study of the Operational Properties of Bistable Smectic-A Liquid Crystal Displays," *Latvian Journal of Physics and Technical Sciences*, vol. 55, no. 3, pp. 54–62, 2018.

[141] M. Maltisovs and D. Pikulins, "Study of Electrical Properties of Bistable Smectic-A Liquid Crystal Displays," *Latvian Journal of Physics and Technical Sciences*, vol. 56, no. 5, pp. 3–11, 2019.

[142] H. Aoki, "Dynamic characterization of a-Si TFT-LCD pixels," *IEEE Transactions on Electron Devices*, vol. 43, no. 1, pp. 31–39, 1996.

[143] B. Bahadur, *Liquid Crystals — Applications and Uses, Vol. 1.* Singapore: World Scientific Pub Co Inc., 1990. [Online]. Available: https://www.worldscientific.com/worldscibooks/10.1142/1013

[144] T.-H. Choi, S.-M. Do, B.-G. Jeon, and T.-H. Yoon, "Low-power control of haze using a liquid-crystal phase-grating device with two-dimensional polymer walls," *Optics Express*, vol. 27, no. 3, p. 3014, 2019.

[145] M. R. Costa, R. A. Altafim, and A. P. Mammana, "Electrical modeling of liquid crystal displays-LCDs," *IEEE Transactions on Dielectrics and Electrical Insulation*, vol. 13, no. 1, pp. 204–209, 2006.

[146] R. Gotlaufs, "Electrically Controllable Optical Diffusers and Development of an Improved Electrical Drive Circuit." Master's thesis, Riga Technical University, 2018.

[147] G. Karmakar, S. Roy, G. Chattopadhyay, and Z. Xiao, "Dynamically controlling exterior and interior window coverings through IoT for environmental friendly smart homes," *Proceedings - 2017 IEEE International Conference on Mechatronics, ICM 2017*, pp. 487–491, 2017.

[148] C. Neusel and G. A. Schneider, "Size-dependence of the dielectric breakdown strength from nano- to millimeter scale," *Journal of the Mechanics and Physics of Solids*, 2014.

[149] J. Naruševiča, "Ventspilī rada gudros logus," pp. 1–1, may 2017. [Online]. Available: https://www.ventasbalss.lv/zinas/brivosta/33140-ventspili-rada-gudros-logus

[150] "Gudro logu prototipu var apskatīt Kurzemes Democentrā," pp. 1–1, may 2017. [Online]. Available: https://www.kurzemesdemocentrs.lv/lv/jaunumi/gudro-logu-prototipu-var-apskatit-kurzemes-democentra/

[151] S. Filatov, "Ventspils: the technological center of Latvia with space ambitions," pp. 1–1, nov 2017. [Online]. Available: https://baltic-review.com/ventspils-technological-center-latvia/

[152] U. Salenieks, "EC Grant Agreement Number: 646155 Funded under: H2020-EU.2.1.2.1.-Developing next generation nanomaterials, nanodevices and nanosystems," EuroLCDs, Riga, Tech. Rep., may 2017. [Online]. Available: www.nano-inspired.eu

[153] M. Esfahani, "Lumotune Glass Display," sep 2017. [Online]. Available: https://www.youtube.com/watch?v=RO1jgPOqoSE

[154] "Lumotone Bi-stable Transparent Display," aug 2017. [Online]. Available: https://www.youtube.com/watch?v=5fw9vDdBFys

APPENDICES

8x1 design *SmA LC* cell recommended functional parameters

Switching voltage (scatter)	13 V/µ (195 V)
Switching voltage (transparent)	9 V/µ (135 V)
Switching waveform	DC balanced square wave
Scatter state frequency	30 Hz
Transparent state frequency	600 Hz
Switching time (scatter)	7.5 s
Switching time (transparent)	1.5 s
Pause between pixel-pixel	1 s
Pause between state-state	5 s
Pause between cycles	5 min

2x2 and 5x5 design *SmA LC* cell recommended functional parameters

Switching voltage (scatter)	12 V/µ (180 V)
Switching voltage (transparent)	9 V/µ (135 V)
Switching waveform	DC balanced square wave
Scatter state frequency	30 Hz
Transparent state frequency	600 Hz
Switching time (scatter)	5 s
Switching time (transparent)	1.5 s
Pause between pixel-pixel	1 s
Pause between state-state	5 s
Pause between cycles	5 min

Numeric design *SmA LC* cell recommended functional parameters

Switching voltage (scatter)	8 V/μ (120 V)
Switching voltage (transparent)	7 V/μ (105 V)
Switching waveform	DC balanced square wave
Scatter state frequency	30 Hz
Transparent state frequency	600 Hz
Switching time (scatter)	3 s
Switching time (transparent)	1 s
Pause between pixel-pixel	1 s
Pause between state-state	5 s
Pause between cycles	2 min

High quality, pixel density (1x1mm pixel size) design

SmA LC cell recommended functional parameters

Switching voltage (scatter)	6 V/µ (90 V)
Switching voltage (transparent)	5.7 V/µ (85.5 V)
Switching waveform	DC balanced square wave
Scatter state frequency	30 Hz
Transparent state frequency	600 Hz
Switching time (scatter)	2 s
Switching time (transparent)	0.5 s
Pause between pixel-pixel	1 s
Pause between state-state	2 s
Pause between cycles	10 min